Journal
of
The Franklin Institute

EDITOR, HENRY BUTLER ALLEN, MET.E., D.Sc.
ASSISTANT EDITOR, JOHN FRAZER, PH.D.

Associate Editors:

WILDER D. BANCROFT, PH.D.
C. B. BAZZONI, PH.D.
ARTHUR L. DAY, SC.D.
R. EKSERGIAN, PH.D.
A. S. EVE, F.R.S.
PAUL D. FOOTE, PH.D.
W. J. HUMPHREYS, PH.D.
C. E. K. MEES, D.SC.
WILLIAM B. MELDRUM, PH.D.
HENRY C. SHERMAN, SC.D.
W. F. G. SWANN, D.SC.
HUGH S. TAYLOR, D.SC.
A. F. ZAHM, PH.D.
JOHN ZELENY, PH.D.

Committee on Publications:

G. H. CLAMER, CHAIRMAN
RICHARD HOWSON
C. L. JORDAN
LIONEL F. LEVY
MALCOLM LLOYD, JR.
HIRAM S. LUKENS
RICHARD H. OPPERMANN
WINTHROP R. WRIGHT

Vol. 245 **JANUARY, 1948** **No. 1**

CONTENTS

Ultrasonic Delay Lines. I. . . H. B. HUNTINGTON, A. G. EMSLIE, AND V. W. HUGHES 1

An Integral-Equation Approach to Problems of Vibrating Beams. Part I. WALTER T. WHITE 25

Visual Measurements of Short Pulses of Direct Current . . . . . PHILIP F. ORDUNG 37

Rigorous and Approximate Treatment of Long Line Transmission Problems by Hyperbolic Functions . . . . . S. GERSZONOWICZ 53

Notes from the National Bureau of Standards 67

The Franklin Institute Notes 73

Notes from the Biochemical Research Foundation 78

Enzymatic Hydrolysis of Desoxyribonucleic Acid Prepared with the Use of Strong Sodium Hydroxide . . . . . CHARLES A. ZITTLE

Book Reviews 81

Publications Received 84

Current Topics 24, 52, 85

Published by
THE FRANKLIN INSTITUTE OF THE STATE OF PENNSYLVANIA
Prince and Lemon Streets, Lancaster, Penna., and
Benjamin Franklin Parkway at Twentieth St., Philadelphia 3, Penna.

DOMESTIC—EIGHT DOLLARS PER YEAR FOREIGN—NINE DOLLARS PER YEAR
(Foreign Postage Additional)
SINGLE NUMBERS—ONE DOLLAR EACH
REPRINTS—FIFTY CENTS PER INDIVIDUAL INSTALLMENTS

Indexes to the semi-annual volumes of the JOURNAL are published with the June and December numbers

V.
19

Journal
of
The Franklin Institute
Devoted to Science and the Mechanic Arts

Vol. 245 JANUARY, 1948 No. 1

ULTRASONIC DELAY LINES. I.*

BY

H. B. HUNTINGTON,† A. G. EMSLIE‡ AND V. W. HUGHES,§

Massachusetts Institute of Technology,
Cambridge, Massachusetts.

ABSTRACT.

This paper, the first of two dealing with ultrasonic delay lines, is concerned mainly with the theoretical considerations involved in the general process of ultrasonic propagation. The transducer action is given considerable attention and an equivalent circuit employing a transmission line as an element is demonstrated. The diffraction spreading of the beam and absorptive losses in the transmitting medium are also discussed.

A. INTRODUCTION.

This paper and its sequel give an account of that research on ultrasonics which was carried out at the Radiation Laboratory at M. I. T. on the development of ultrasonic delay lines. In this paper will be presented some of the general theoretical considerations which are involved in such a device and in the second paper the construction and operation of the actual delay line is treated from the experimental standpoint.

An ultrasonic delay line functions by transforming an electrical signal into a sonic one by an electromechanical transducer, propagating it through a fixed path in the transmitting medium and then converting the sonic signal back into an electrical signal by a second transducer. Very long delays can be obtained by this method, in comparison to purely electrical devices, because of the greatly decreased velocity of sound as compared to the velocity of electromagnetic propagation. Since the velocity of sound in liquids is about a third of that in solids,

* This paper is based on work done for the Office of Scientific Research and Development under Contract OEMsr-262 with the Massachusetts Institute of Technology.

† Now at Rensselaer Polytechnic Institute, Troy, New York.

‡ Now at Williams College, Williamstown, Massachusetts.

§ Now at Columbia University, New York, New York.

(Note—The Franklin Institute is not responsible for the statements and opinions advanced by contributors in the JOURNAL.)

a good deal of the research has been on liquid delay lines. However, some promising results have been obtained with multiply reflected beams in solids.

The frequency response of an ultrasonic delay line has a maximum at the resonant frequency of the quartz crystals and falls off at low frequencies. Therefore, it is necessary, in order to obtain undistorted transmission of pulses, to send the pulses through the line on a carrier whose frequency is near that of the crystals. This allows exceedingly faithful transmission. In some cases, however, the wave shape of the transmitted pulse is not so critical provided a rapid rate of rise is maintained. This is true when it is desired to delay a trigger pulse and therefore a trigger line can be operated without a carrier.

B. TRANSDUCER ACTION AND LOSS THROUGH MISMATCH.

The treatment of this section deals with the analysis of the fundamental action of the piezoelectric transducer, operating in the thickness vibration. The results deduced here are subsequently referred in another paper and form the basis for approach to many design problems in ultrasonic devices. As such these results are by no means original with the present group but the presentation differs somewhat from those already in the literature. The general plan has been to attack the problem directly by fundamental procedure, making use of assumptions and approximations valid for the situations under consideration but avoiding equivalent circuits which hold only over a limited range of frequency. From fundamental equations an expression for the impedance of the transducer is obtained as seen from the external driving circuit. Transformation of the impedance in series with the electrostatic capacity to a shunt admittance is then carried out and certain small terms are neglected. The behavior of the circuit at resonance is investigated.

At this point a somewhat more general treatment is introduced to show that, if the fundamental equations are written so that they express the current-voltage relations in a six-terminal network and the same approximation is made on transforming from a series to a shunt circuit, there exists a very simple equivalent circuit involving a transmission line section. This circuit is then a general statement of all the specific results which have been derived earlier.

The next paragraphs investigate the frequency response of the transducer. The behavior near resonance is analyzed in terms of an equivalent "Q."

The last part of this section is concerned with the calculation of the loss in energy transfer arising from impedance mismatch. For broad band performance the electrical circuits on both driving and receiving crystals must be loaded with resistors of a few hundred ohms. On the other hand, the transducers usually present impedances of the order of

several kilohms. Some consideration is given to the choice of crystal diameter for least loss, keeping bandwidth constant. The possibilities in driving the crystal at higher harmonics are also discussed.

The first step will be the development of an expression for the electrical impedance of the transducer in terms of acoustic impedances. Consider a piezoelectric crystal of uniform thickness fitted across a tube of uniform cross section and bounded by media 1 and 2 respectively, at opposite faces (see Fig. 1).

The case considered is that of vibration propagated in the thickness (x) direction as for example, in X-cut quartz. It will be assumed that no other modes are appreciably excited and that the displacements depend only on the x-coordinate. The dimensions of the vibrating crystal surfaces are large compared to the wavelength of the vibration. No acoustic reflection is returned from objects in the media during the time of excitation. One would like to know what is the equivalent electrical circuit as seen looking at terminals attached respectively to the electrodes on the crystal faces.

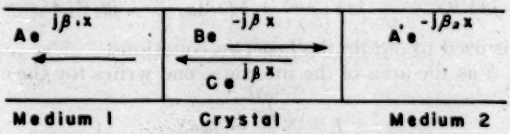

FIG. 1. Vibrating crystal loaded on both sides.

The appropriate equations for the piezoelectric medium are [1]

$$s = Y\frac{\partial \xi}{\partial x} + h\frac{D}{4\pi} \tag{1}$$

$$E = h\frac{\partial \xi}{\partial x} + \frac{D}{K}, \tag{2}$$

where ξ = displacement of the mechanically vibrating medium,
s = stress,
Y = the appropriate modulus of elasticity,
D = the electrical displacement $= 4\pi\sigma$,
σ = the free charge per unit area of the electrodes,
E = electric field
K = dielectric constant of the crystal,
h = piezoelectric coefficient appropriate to the independent variables used and the orientation of the crystal.

It should be remarked that Y, h and K are functions of the orientation of the crystal.

[1] "Electromechanical Transducers and Wave Filters," W. P. Mason, Van Nostrand, pp. 202, 231 (1942); NDRC Report 14–271, W. Swann.

When the crystal is electrically excited at a frequency $\omega/2\pi$, nearly plane waves are propagated outward from both interfaces with wavelengths of $2\pi/\beta_1$ and $2\pi/\beta_2$, respectively (see Fig. 1). In the adjacent media the stress is given by $S = Y_{1 \text{ or } 2}(\partial\xi/\partial x)$. Inside the crystal, waves will be moving in both directions. (It will be our practice throughout these articles to consider that the time dependent factor, $e^{j\omega t}$, is implicitly contained in the amplitude coefficient.) One is able to assign a definite wavelength to the propagation inside the crystal by virtue of the fact that the quantity $hD/4\pi$ in (1) is independent of x.

The boundary conditions are that the mechanical displacement and pressure be continuous. This gives four equations for the four k unknown amplitude coefficients:

$$A = B + C, \tag{3a}$$

$$Be^{-j\beta d} + Ce^{j\beta d} = A'e^{-j\beta_2 d}, \tag{3b}$$

$$j\beta_1 Y_1 A = -j\beta YB + j\beta YC + hD/4\pi, \tag{3c}$$

$$-j\beta YBe^{-j\beta d} + j\beta YCe^{j\beta d} + hD/4x = -j\beta_2 Y_2 A'e^{-j\beta_2 d}, \tag{3d}$$

where (1) is used to obtain the last two equations.

Taking S as the area of the interface, one writes for the current

$$I = S\frac{d\sigma}{dt} = j\omega\sigma S, \tag{4}$$

where (σ) is free change per unit area of the electrodes. For the voltage across the crystal measured in the sense of Ohm's Law, one obtains from equation (2)

$$V = +\int_0^d Edx = h(\xi_d - \xi_0) + \frac{4\pi\sigma d}{K}. \tag{5}$$

The equations (3) can be solved for displacements in the usual way and give

$$\begin{aligned}\xi_d &= A'e^{-j\beta_2 d} \\ &= jh\sigma \frac{\beta Y\{\cos(\beta d) - 1\} + jY_1\beta_1 \sin\beta d}{(\beta Y)(\beta_1 Y_1 + \beta_2 Y_2)\cos\beta d + j[(\beta Y)^2 + \beta_1 Y_1 \beta_2 Y_2]\sin\beta d} \qquad (6a) \\ &= jh\sigma F_2(\beta d),\end{aligned}$$

$$\begin{aligned}-\xi_0 &= -A \\ &= jh\sigma \frac{\beta Y\{\cos(\beta d) - 1\} + jY_2\beta_2 \sin\beta d}{(\beta Y)(\beta_1 Y_1 + \beta_2 Y_2)\cos\beta d + j[(\beta Y)^2 + \beta_1 Y_1 \beta_2 Y_2]\sin\beta d} \qquad (6b) \\ &= jh\sigma F_1(\beta d).\end{aligned}$$

The expression for the electrical impedance of the crystal can now be

written

$$\frac{V}{I} = \frac{4\pi d}{j\omega K S_1} + \frac{h^2}{\omega S} F(\beta d), \tag{6c}$$

where

$$F = F_1 + F_2. \tag{6d}$$

The first term in (6c) is always much larger than the second, provided that at least one of the media adjoining the crystal is either a

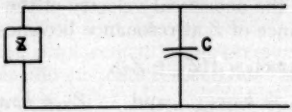

FIG. 2. Shunt circuit.

liquid or a solid. This makes it feasible to express the transducer as a simple parallel combination.

$$I/V = j\omega C + (Z)^{-1} \tag{7}$$

Here C is the electrostatic capacity of the crystal and

$$Z = \frac{16\pi^2 d^2}{h^2 K^2 \omega S F(\beta d)} \tag{7a}$$

is the equivalent electrical impedance of the crystal under the above conditions of acoustical loading (see Fig. 2). The approximation implicit in (7) greatly simplifies the subsequent treatment and the results check closely with the more exact calculation. For example, the

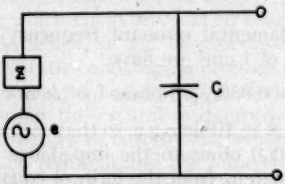

FIG. 3. Circuit with generator.

resonant frequency of the transducer as developed here differs by less than 1 per cent. from the exact value.

From (6c) it is apparent that the electrostatic capacity of the crystal acts as a series element. This is a consequence of the fact that the thickness vibration is being considered. (Where the direction of the supersonic waves is at right angles to the electric field the electrostatic capacity appears as a shunt element.)

If one had developed the case of the receiving rather than the transmitting crystal, an impinging acoustical wave would have been introduced. Then the equivalent electrical circuit would have involved a generator, with voltage amplitude proportional to the amplitude of the incoming sonic wave (see Fig. 3).

The resonant condition for the crystal is that its width be an odd number of half wavelengths, or $\beta d = n\pi$ where n is odd. At these values F (see 6) reduces to $4(\beta_1 Y_1 + \beta_2 Y_2)^{-1}$. Since $Y = v^2\rho$ where ρ is the density and v the acoustical velocity of the excited mode in the medium, the impedance of Z at resonance becomes

$$Z(n\pi) = \tfrac{1}{4}(Z_1 + Z_2), \tag{8}$$

$$Z_1 = k\rho_1 v_1 \quad \text{and} \quad Z_2 = k\rho_2 v_2.$$

The quantity k is given by

$$k = \left(\frac{4\pi d}{hK}\right)^2 \frac{1}{S}. \tag{8a}$$

Since ρv is the acoustical impedance of a medium, k is the proportionality factor between electrical and acoustical impedance. The quantity k depends entirely on the characteristics of the crystal alone, i.e. its dimensions and its electric and piezoelectric properties. For an X-cut quartz crystal

$$K = 4.58,$$
$$h = 14.3 \times 10^4 \text{ c.g.s. e.s.u.}$$

and

$$d \text{ in mm.} = \frac{2.86 \times 10^6}{f},$$

where f is the fundamental resonant frequency. For a 30 mc./sec. crystal with an area of 1 cm^2. we have

$$Z_1 = 0.030(\rho_1 v_1) \text{ ohms for } (\rho v \text{ in c.g.s.}).$$

For mercury ρv is 19.8×10^5 in c.g.s. so that each quartz mercury interface contributes 15,000 ohms to the impedance of the transducer at resonance. It is apparent from the form of equation (8) that at resonance the two bounding media act as series elements.

From the direct approach employed in the preceding paragraphs, an expression for the impedance of the transducer, looking in from the electrical side, has been obtained. Its behavior at resonance has been investigated. A proportionality factor between electrical and acoustical impedance has been evolved and some actual numbers inserted. Also, expressions have been derived for the displacement amplitudes at the interfaces (equation 6a and 6b) in terms of the free charge on the crystal. A somewhat more general approach to the fundamental

equations will now be employed with a view to obtaining a compact equivalent circuit from which any specific result could be derived.

One starts from equations (3) using parts (a) and (b) to eliminate B and C from parts c and d. The new equations are

$$\omega\rho_1 v_1 A = j\omega\rho v(A \cot \beta d - A' e^{-j\beta_2 d} \csc \beta d) - \frac{h}{\omega S} I, \tag{9a}$$

$$\omega\rho_2 v_2 A' e^{-j\beta_2 d} = j\omega\rho v(-A \csc \beta d + A' e^{-j\beta_2 d} \cot \beta d) + \frac{h}{\omega S} I. \tag{9b}$$

Next one identifies the displacements and pressures at the interfaces with fictitious voltages and currents respectively, as follows:

$$A = -e_1/h, \qquad A' e^{-j\omega_2 d} = e_2/h,$$

$$\omega\rho_1 v_1 A = \frac{h}{\omega S} i_1, \qquad \omega\rho_2 v_2 A' e^{-j\beta_2 d} = \frac{h}{\omega S} i_2. \tag{10}$$

The substitution of these quantities into 9a, 9b and 5 gives the following three equations:

$$\frac{h^2}{j\omega^2\rho v S}(i_1 - I) = e_1 \cot(\beta d) + e_2 \csc(\beta d),$$

$$\frac{h^2}{j\omega^2\rho v S}(i_2 - I) = e_1 \csc(\beta d) + e_2 \cot(\beta d), \tag{11}$$

$$V = e_1 + e_2 + \frac{4\pi d I}{jk\omega S}.$$

These equations give the relations between the voltages and currents in a six-terminal network which could serve as an exact equivalent circuit for the transducer. As before, it will be expedient to change from a circuit where the electrostatic condenser is in series to one in which the condenser is in parallel and to neglect terms of the order of $(\omega c Z)^{-2}$, which is permissible when the crystal is damped. In the equations for the new network the roles of current and voltage in equation (11) are interchanged at each terminal and the impedance factors, such as $h^2/\omega^2\rho v S$, are multiplied by $(kS/4\pi d)^2$ and become admittances. Consequently, the new network equations are

$$(e_1 - V) = jZ_0[i_1 \cot(\beta d) + i_2 \csc(\beta d)],$$

$$(e_2 - V) = jZ_0[i_1 \csc(\beta d) + i_2 \cot(\beta d)], \tag{12}$$

$$I = i_1 + i_2 = \frac{j\omega k S}{4\pi d} V,$$

where $Z_0 = k\rho v$, the equivalent electrical impedance of the quartz.

Equations (12) can be represented by the equivalent circuit shown in Fig. 4, which first appeared in a report by H. Grayson.[2] Here the crystal is represented as a section of a transmission line (see the two parallel heavy lines) of electrical length βd and characteristic impedance Z_0. By tying on impedances Z_1 and Z_2, to the appropriate terminals, one can now rederive the specific results obtained in the first part of this section.

The next problem is the investigation of the band-pass characteristics of the crystal. From the analytical expression for Z (6 and 7) one obtains the following formula for conductance,

$$G = Re\left(\frac{1}{Z}\right) = \frac{\{Z_0^2(\cos(\beta d) - 1)^2 + Z_1 Z_2 \sin^2 \beta d\}(Z_1 + Z_2)}{Z_0^2(Z_1 + Z_2)^2 \cos^2(\beta d) + [(Z_1 Z_2 + Z_0^2)\sin \beta d]^2}. \quad (13)$$

This quantity (13) is proportional to the power (V^2G) absorbed by one crystal from a constant voltage source. The frequency response is obtained by varying βd. Figure 5 shows the behavior of (13) under four different conditions. All curves are periodic with period 2π for βd. When the crystal is acoustically matched on both sides, the curve is sinusoidal (A). The curve is narrowed somewhat (B) as the result of allowing one surface to vibrate freely ($Z_2 = 0$). If one employs a material of higher acoustical impedance on both sides ($Z_1 = Z_2 = \sqrt{2}Z_0$), a broader curve is obtained (C). Curve D is obtained when one of these surfaces is allowed to vibrate freely ($Z_2 = 0$) and shows a zero curvature at resonance, nearly the case of quartz with mercury on one side. This final result is somewhat unexpected and is of practical interest.

The expression (13) gives the *total* power absorbed by the crystal. For the two special cases considered above ($Z_1 = Z_2$, and $Z_2 = 0$) there is no question how the power is divided between the two media. Though these are two situations of main practical concern, it is of interest to determine how the power is divided in the general case. To do this, we must return to equation (6) to evaluate the ratio

$$Y_1\left|\xi_0 \frac{\partial \xi_0}{\partial x}\right| : \quad Y_2\left|\xi_d \frac{\partial \xi_d}{\partial x}\right|.$$

This turns out to be

$$\frac{\text{Power transmitted to medium 1}}{\text{Power transmitted to medium 2}} = \frac{Z_1 Z_2^2 \sin^2(\beta d) + Z_0^2 Z_1 [\cos(\beta d) - 1]^2}{Z_1^2 Z_2 \sin^2(\beta d) + Z_0^2 Z_2 [\cos(\beta d) - 1]^2}. \quad (14)$$

It follows that the power absorbed by the medium 1 from a voltage

[2] "The Quartz Crystal as a Generator and Receiver of Supersonic Vibration," H. Grayson, TRE Report T-1358.

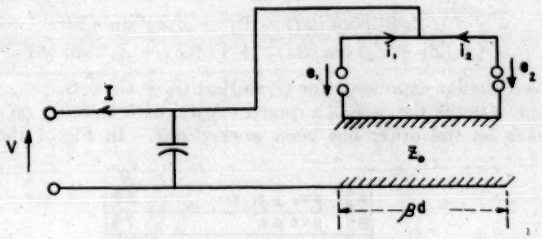

FIG. 4. Transmission-line equivalent circuit.

		"Q"
A	$\rho_1 v_1 = \rho v = \rho_2 v_2$	.79
B	$\rho_1 v_1 = \rho v;\ \rho_2 v_2 = 0$	1.11
C	$\rho_1 v_1 = \sqrt{2}\,\rho v = \rho_2 v_2$	.56
D	$\rho_1 v_1 = \sqrt{2}\,\rho v;\ \rho_2 v_2 = 0$	0

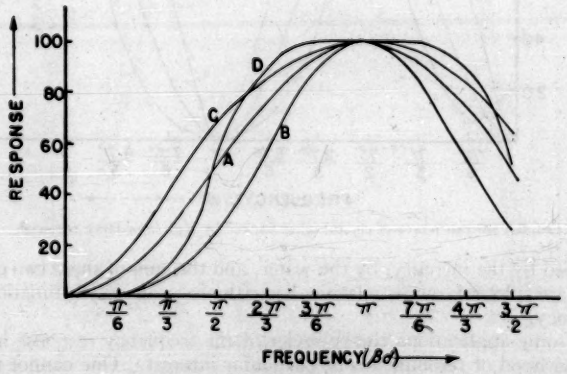

FIG. 5. Acoustic output power of a crystal as a function of frequency. The crystal is assumed to be subject to a constant voltage. Fig. 1 gives meaning of subscripts. Resonant frequency of free crystal occurs for $\beta d = \pi$. "Q" refers to curvature at resonance.

source is proportional to

$$G_1 = \frac{Z_0^2 Z_1 [\cos(\beta d) - 1]^2 + Z_1 Z_2^2 \sin^2(\beta d)}{[Z_0(Z_1 + Z_2)\cos(\beta d)]^2 + [(Z_1 Z_2 + Z_0^2)\sin(\beta d)]^2}. \quad (15)$$

There is a similar expression for G_2 so that $G_1 + G_2 = G$.

As an example the case of a quartz crystal with mercury on one side and water on the other has been worked out. In Fig. 7 the power

		"Q"
A	$\rho v = 2\rho_1 v_1$	.39
B	$\rho v = \rho_1 v_1$	.79
C	$\rho v = \frac{1}{2}\rho_1 v_1$	1.57

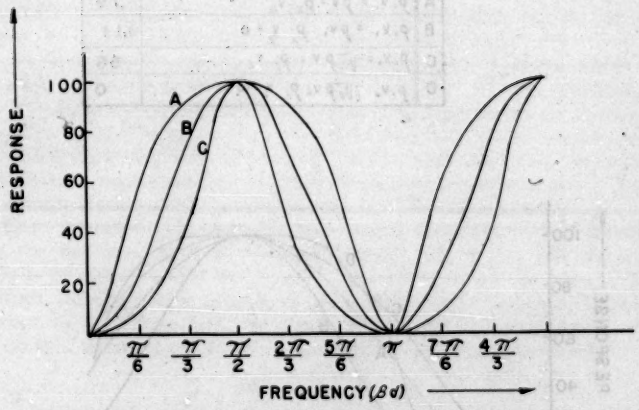

FIG. 6. Output power of crystal when backed by high impedance material.

absorbed by the mercury, by the water, and the sum of these two quantities are plotted on a relative logarithmic scale as a function of frequency.

In some applications the behavior of the frequency response in the neighborhood of resonance is of particular interest. One cannot use a simple series resonant circuit to represent both the amplitude and phase characteristics accurately here even over a limited frequency range. However, it is convenient to introduce a parameter, "Q," which is the Q value for the simple series resonant circuit whose amplitude response matches that of the transducer in curvature at resonance.

For all but the lowest values, the parameter "Q" corresponds satisfactorily with the usual ratio of mid-frequency to distance between half power points. The formula for "Q" is given below and applies to

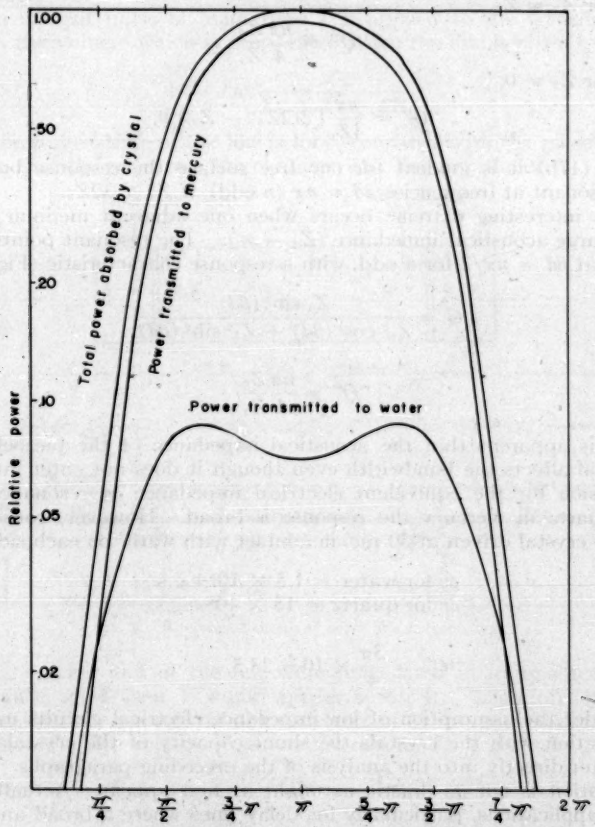

FIG. 7. Frequency response; quartz crystal loaded with mercury on one side, water on the other.

the curve for power absorbed by the transmitting medium when the transmitter crystal is driven from a low impedaance.

$$"Q" = \frac{n\pi}{4}\left[\frac{4(Z_1Z_2 + Z_0^2)^2 - (Z_1 + Z_2)^2(Z_2^2 + 2Z_0^2)}{Z_0^2(Z_1 + Z_2)^2}\right]^{\frac{1}{2}}, \qquad (16)$$

where medium 1 is the transmitting medium. Here n is the order of the harmonic frequency of the crystal. For special cases the following simplifications occur:

For $Z_1 = Z_2$,

$$"Q" = \frac{n\pi}{4}\frac{Z_0}{Z_1}, \tag{17a}$$

and for $Z_2 = 0$,

$$"Q" = \frac{n\pi}{4Z_1}[2(2Z_0^2 - Z_1^2)]^{\frac{1}{2}}. \tag{17b}$$

From (17b) it is evident for one free surface the response becomes antiresonant at frequencies $\beta d = n\pi$ (n odd), if $Z_1 > \sqrt{2}Z_0$.

An interesting extreme occurs when one adjacent medium has a very large acoustical impedance ($Z_2 \to \infty$). The resonant points then occur at $\beta d = n\pi/2$ for n odd, with a response characteristic (Fig. 6).

$$G = \frac{Z_1 \sin^2(\beta d)}{Z_0^2 \cos^2(\beta d) + Z_1^2 \sin^2(\beta d)} \tag{18}$$

and

$$"Q" = \frac{n\pi}{4}\frac{Z_0}{Z_1}.$$

It is apparent that the acoustical impedance of the piezoelectric material affects the bandwidth even though it does not enter into the expression for the equivalent electrical impedance at resonance (8). For quartz in mercury the response is broad. However, consider a 10 mc. crystal driven at 30 mc. in contact with water on each side.

$$\rho v \text{ for water} = 1.5 \times 10^5 \text{ c.g.s.},$$
$$\rho v \text{ for quartz} = 15 \times 10^5 \text{ c.g.s.},$$

then

$$"Q" = \frac{3\pi}{4} \times 10 = 23.5.$$

Under the assumption of low-impedance electrical circuits used in conjunction with the crystals the shunt capacity of the crystals does not enter directly into the analysis of the preceding paragraphs. This assumption is not as drastic as might at first appear. Actually for many applications, particularly for delay lines where a broad and flat passband is desired, the crystal capacity is an element in a low-Q shunt resonant circuit. The impedance of this circuit is kept low in comparison with Z_1, Z_2, etc. by the bandwidth requirements. Under these circumstances the results of the last paragraphs are quite valid.

It remains to calculate the actual loss through mismatch that occurs where a signal is transmitted through a delay line as depicted in Fig. 8. The equivalent circuit is given in Fig. 9. The load resistors shunting

the crystals at the transmitting and receiving ends are R_t and R_r, respectively. Consider the crystals' capacities as tuned out. (The resolution of Z into two series elements $\frac{1}{4}Z_1$ and $\frac{1}{4}Z_2$ is possible only at resonance.)

If a current pulse of magnitude I is applied to the transmitting crystal, the voltage which is propagated down the line is given by

$$V = IR_t \frac{Z_1}{Z_1 + Z_2 + 4R_t}. \tag{19}$$

Here the transit time of the line is long compared with the pulse duration, so that the pulse sees the characteristic line impedance.

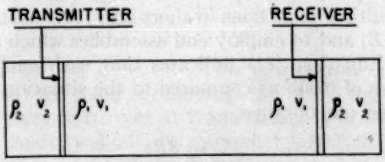

FIG. 8. Delay line schematic.

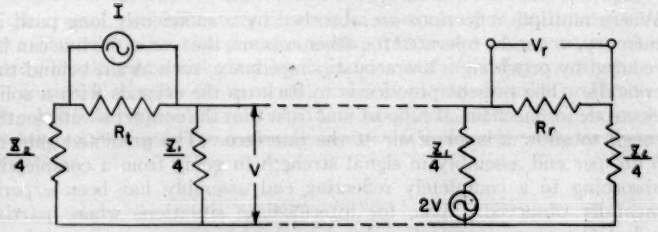

FIG. 9. Equivalent circuit of delay line at resonance.

If the other end of the line were terminated in its characteristic impedance, $Z_1/4$ then V would appear across it. Therefore, looking back at the line, one sees a pulse generator of $2V$ in series with the line impedance.[3] The voltage V_r across the resistor R_r is given by

$$V_r = 2V \frac{R_r}{\frac{1}{4}(Z_1 + Z_2) + R_r}$$

$$= IR_t \frac{8Z_1R_r}{(Z_1 + Z_2 + 4R_t)(Z_1 + Z_2 + 4R_r)}. \tag{20}$$

[3] If the crystals at the two ends of the line differ with respect to any of the quantities upon which k (eq. 8a) depends, then Z_1 will have different values at the two ends, say Z_1' and Z_1''. If we require that the available power be transformed without reflection by the line, then equation (20) is valid (with appropriate superscripts in the denominator) if Z_1 in the numerator is replaced by the geometric mean of Z_1' and Z_1''.

As has been remarked before, R_t and R_r can generally be neglected in comparison with Z_1 and Z_2. The ratio of output to input voltage can then be simplified accordingly

$$V_r/IR_t = \frac{8Z_1R_r}{(Z_1 + Z_2)^2}. \tag{21}$$

The corresponding power ratio is to the same degree of approximation,

$$\frac{R_tR_r(8Z_1)^2}{(Z_1 + Z_2)^4}.$$

For $R_r = R_t$ the power loss equals the voltage loss.

To avoid multiple reflections in short lines, it is customary to try to make Z_2 equal Z_1 and to employ end assemblies which absorb the incident energy. Equation (21) indicates that each such end assembly introduces a loss of 6 db. as compared to the situation where Z_2 is set equal to zero and one obtains

$$\frac{V_r}{IR_t} = \frac{8R_r}{Z_1}. \tag{22}$$

Where multiple reflections are absorbed by a sufficiently long path in mercury, or can be tolerated for other reasons, the loss in the line can be reduced by providing a low acoustic impedance, such as air, behind the crystals. The present practice is to back up the crystals with a solid electrode for mechanical support and trust that the contact is sufficiently rough to allow a layer of air at the interface. The predicted gain of 6 db. per end assembly in signal strength in going from a completely absorbing to a completely reflecting end assembly has been experimentally observed. Also, for intermediate situations where partial reflection at an imperfectly absorbing back-surface, experimental results were consistent with equation (21).

The mismatch loss predicted by equation (22) has been experimentally verified for a tube of nearly one inch diameter. For smaller tubes the loss was greater than would be expected and might be due to mechanical edge effects at the periphery of the crystals. With a tube of $\frac{1}{4}''$ ID the measured loss was about 10 db. more than predicted. With a tube of $25/64''$ ID the measured loss was found to be 6 db. more than predicted.

The formulae developed here can be used to help choose optimum values for certain parameters. Two applications will be considered here, the choice of active crystal area and choice of fundamental or of harmonic frequency for the crystal operation. One desires to obtain the maximum ratio of output voltage to input current for constant bandwidth. In both cases the capacity at each crystal will be composed of two parts, a stray capacity C, which should be kept to a minimum and

a live capacity $C_l = kS/4\pi d$, where S is the area of the crystal actively excited. The values of R_t and R_r must be inversely proportional to $(C_s + C_l)$ if the bandwidth is to be maintained constant. The quantity we wish to maximize has already been shown to be

$$\frac{V_r}{I} = \frac{8Z_1R_rR_t}{(Z_1 + Z_2)^2}. \tag{21a}$$

For the determination of optimum crystal area S we note that Z_1 and Z_2 vary inversely as S (Eq. 8*a*). Under the conditions of varying S and holding d constant, the Z's vary inversely as C_l. It follows that

$$\frac{V_r}{I} \sim \frac{C_l}{(C_s + C_l)^2}, \tag{21b}$$

which as a maximum for $C_l = C_s$. This means that one chooses the crystal area so that live capacity matches the stray, for optimum ratio of voltage at receiver to current at transmitter. For optimum signal-to-noise the line capacity should be somewhat larger, depending on the characteristics of the amplifier's first stage.

Since, for constant S, the C_l decreases with the resonant frequency of the crystal, excessive stray capacity is more costly at lower frequencies: The reason for this paradox is that the lower the frequency the more difficult it is to make the line capacity match a fixed stray capacity.

To decide whether fundamental or harmonic operation is preferable one varies the crystal thickness d holding S constant. The Z's vary directly as d^2 (Eq. 8a) or inversely as C_l^2. It follows that under these conditions

$$\frac{V_r}{I} \sim \frac{C_l^2}{(C_s + C_l)^2}. \tag{21c}$$

This means one wants the largest live capacity possible in this case, in other words, operation of the crystal on the fundamental frequency. For a given frequency the crystal that operates on the fundamental is the thinnest crystal that can be used. It is of interest to note that, if the stray capacity were negligible, working on the harmonics would correspondingly involve no additional loss.

In the preceding analysis the driving and receiving circuits have been represented simply by a tuning coil and loading resistor in parallel. In any actual application the loss through mismatch can be reduced by a transforming network. Because of the bandwidth requirements, however, it is often impractical to use as high a transformation ratio as would be required for match and the assumption that Z_1, Z_2, etc. are large compared with the transformed impedance can be made. Up to this time it has not appeared feasible to use an acoustical transformer, particularly in the range of several megacycles.

C. WAVE PROPAGATION.

It is of considerable importance to determine in as great detail as possible the way in which energy travels after leaving the transmitter of a supersonic system. To this end some calculations are first included on the radiation pattern to be expected from a piezoelectric crystal transmitting single-frequency compressional vibrations into a semi-infinite medium. Secondly, we shall make some remarks on the wave pattern present in a semi-infinite cylindrical tube at the end of which a similar crystal is vibrating. The second case corresponds more closely to the actual physical set-up for a delay line, though results obtained from the first case are also of value in determining mechanical tolerances for delay line construction.

Two assumptions in particular which are made in connection with both cases should be noted. First, as is customary in such calculations,

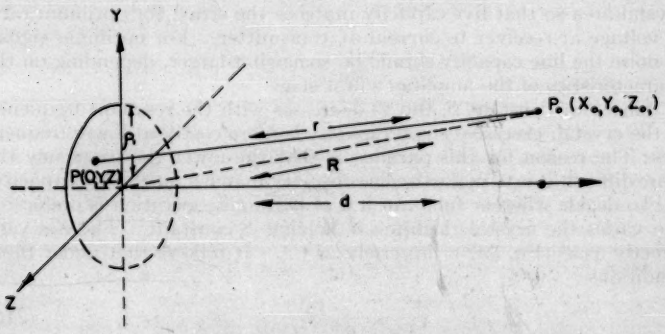

FIG. 10. Geometry of the radiation problem.

we determine the beam pattern in a certain region of "empty" space and then assume that the wave function will remain unchanged if the receiver is placed in this region. This is of course valid for pulse transmission which was our main concern at the Radiation Laboratory. Secondly, we consider that out medium is non-viscous. In the next section of this part, certain effects of viscosity will be considered.

Case I: The Radiation Pattern in a Semi-infinite Medium.

General and Fresnel Case

The nomenclature for the problem is indicated in Fig. 10. A crystal with a circular cross section of radius ρ_1 and with its center at (0, 0, 0) is executing small amplitude, single-frequency vibrations in the direction of the x-axis. The portion of the YZ plane for which $\rho > \rho_1$ is assumed to be a rigid baffle. We wish to know the radiation pattern as

observed at an arbitrary point (X_0, Y_0, Z_0) to the right of the YZ plane.

It is well known that the velocity potential, W, for sound waves of small amplitude in a perfect compressible fluid satisfies the scalar wave equation.[4]

$$\frac{\partial^2 W}{\partial t^2} = v^2 \nabla^2 W, \tag{22a}$$

where v is the velocity. The boundary conditions on the plane $X = 0$ are:

$$\frac{\partial S}{\partial X} = \begin{cases} \text{constant} \neq 0 & (\rho \leq \rho_0) \\ 0 & (\rho > \rho_0). \end{cases} \tag{22b}$$

These boundary conditions neglect the fact that the face of the crystal does not always lie in the same plane. But we shall always calculate the amplitude of the sound wave at a distance from the circular opening which is large compared with the wavelength, and in this case this is a valid approximation. We use the Kirchhoff condition which states: [5]

$$V_0 = \int_{\text{opening}} \frac{\partial W}{\partial n} \frac{1}{r} \sin 2\pi \left(\frac{t}{T} - \frac{r}{\lambda} \right) \cos (nr) d\sigma, \tag{23}$$

where, referring to Fig. 10,

V_0 = velocity at P_0, the observation point,
$\frac{\partial W}{\partial n} = \frac{A}{\lambda}$ in which A is a constant,
λ = wavelength,
T = period.
(nr) = angle between direction of X-axis and r,
t = time variable,
$d\sigma$ = element of area of surface $x = 0$.

Referring to Fig. 10 we see

$$r = R \sqrt{1 + \frac{Y^2 + Z^2 - 2YY_0 - 2ZZ_0}{R^2}}.$$

By analogy to light diffraction problems we distinguish two cases. If it is assumed that r is expanded as

$$r = R \left(1 + \frac{Y^2 + Z^2}{2R^2} - \frac{YY_0 + ZZ_0}{R^2} \right),$$

[4] A. G. Webster, "Dynamics"; Stechert, pp. 542–3 (1922).

[5] For discussion and partial derivation see Stratton's "Electromagnetic Theory," McGraw-Hill, pp. 460–463 (1941). It should be pointed out that our radiation problem resembles that of determining the diffraction pattern to the right of a circular opening upon which a plane wave of light is incident from the left.

we are dealing with the Fresnel case. If

$$r = R\left(1 - \frac{YY_0 + ZZ_0}{R^2}\right)$$

we are dealing with the Fraunhofer case. We consider first the Fresnel case. Hence (23) can be simplified to (24).

$$V_0 = A' \int_{\text{opening}} \sin 2\pi \left(\frac{t}{T} - \frac{r}{\lambda}\right) d\sigma, \tag{24}$$

where

$$A' = \frac{A}{\lambda}\frac{\cos(nR)}{R}.$$

This integral is now in a form which has been evaluated. With the omission of the factor A' the integral can be written as

$$\int_0^{2\pi}\int_0^{\rho_0} \sin 2\pi \left(\frac{t}{T} - \frac{r}{\lambda}\right) \rho d\phi d\rho = M \sin\left(\theta + 2\pi\frac{t}{T}\right), \tag{25}$$

where ρ and ϕ are polar coordinates for the circular opening, M and θ are functions of X_0, Y_0, and Z_0. The elaborate and laborious process of computing M for several values of (X_0, Y_0, Z_0) has been carried through in a paper by E. Lommel on "The Diffraction Phenomena of a Circular Opening and a Circular Screen." [6] These calculations check the experimental data on diffraction of light to within about 1 or 2 per cent.

Fraunhofer Case

The solution of the Fraunhofer problem is well known,[7]

$$M^2 = 4\left[\frac{J_1\left(\frac{2\pi}{\lambda}\rho_1 x\right)}{\left(\frac{2\pi}{\lambda}\rho_1 x\right)}\right]^2, \tag{26}$$

where J_1 is a Bessel function of the first kind and x is the sine of the angle which R makes with the X axis.

On the Axis

An analytical expression for the disturbance on the X-axis for the Fresnel case can be obtained quite readily. By (23) for a plane wave incident normally.

$$V_0 = \frac{A}{\lambda}\int_{\text{opening}} \frac{\sin 2\pi\left(\frac{t}{T} - \frac{r}{\lambda}\right) d\sigma}{r}. \tag{27}$$

[6] E. Lommel, *Abhandlungen der Bayerischen Akademie der Wissenchaften*, **15**, 233 (1886).

[7] M. Born, "Optik," pp. 159–161 (J. Springer, 1933); or P. Morse, "Vibration and Sound," p. 257 (McGraw-Hill, 1936).

This expression is valid so long as $r > \rho_1$. It can be integrated directly with respect to r and gives

$$V_0 = 2A \sin\left(\frac{\pi\rho_1^2}{2\lambda d}\right) \sin 2\pi\left(\frac{t}{T} - \frac{d}{\lambda}\right), \tag{28a}$$

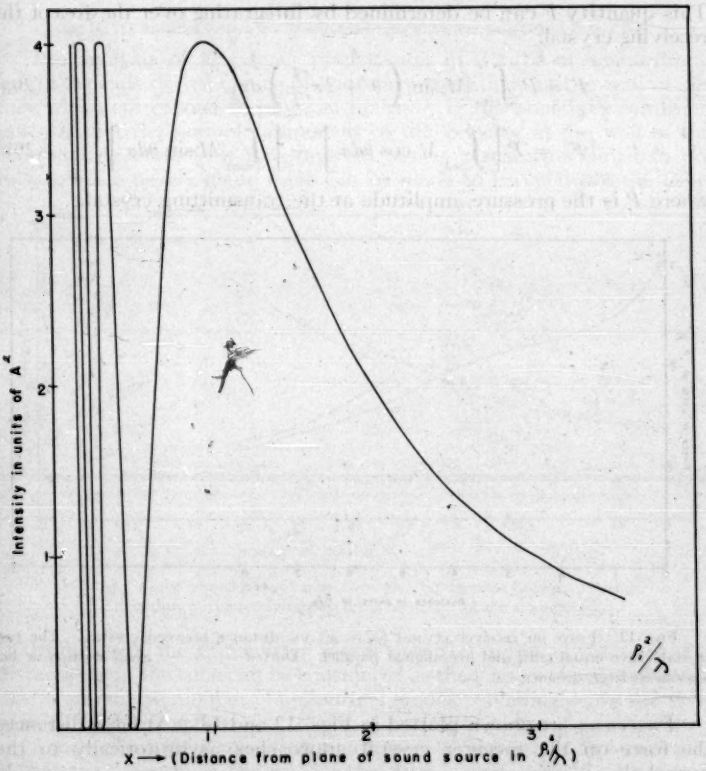

FIG. 11. Intensity of sound on X-axis vs. distance from sound source.

where A is as before the amplitude of the velocity at the crystal. This equation is plotted in Fig. 11. At large distances the amplitude of the velocity reduces to the well-known formula:

$$V_0 = \frac{A_0}{\lambda d}(\pi\rho_1^2). \tag{28b}$$

Total Force on Receiving Crystals

Since the wave incident on our receiver crystal is not a plane wave, pressures of different amplitude and phase will fall at different points of the receiver crystal. It appears that the factor of importance in determining the response of the receiver crystal is the total force on it. This quantity F can be determined by integrating over the area of the receiving crystal.

$$F = P \int_{\text{area}} M \sin\left(\theta + 2\pi \frac{t}{T}\right) d\sigma, \tag{29a}$$

$$|F| = P\left[\int_{\text{area}} M \cos\theta d\sigma\right]^2 + \left[\int_{\text{area}} M \sin\theta d\sigma\right]^2, \tag{29b}$$

where P is the pressure amplitude at the transmitting crystal.

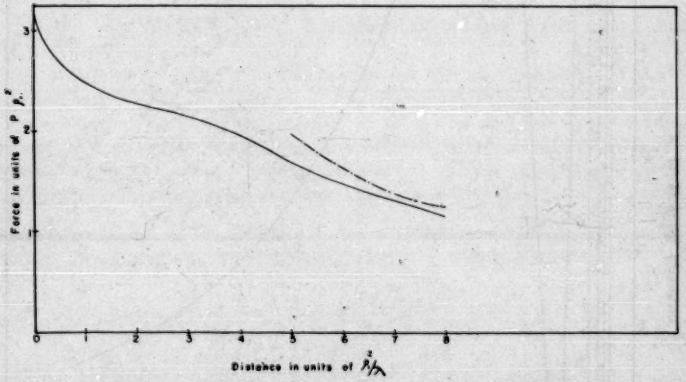

FIG. 12. Force on receiver crystal ($\rho_2 = \rho_1$) vs. distance between crystals. The two crystals have equal radii and are aligned parallel. Dotted —·—·— gives asymptotic behaviour at large distances.

Two cases are shown plotted in Figs. 12 and 13. At large distances the force on the receiver crystal approaches asymptotically to the hyperbola

$$|F| = P \frac{\pi^2 \rho_1^2 \rho_2^2}{\lambda d}, \tag{30}$$

which is also drawn in Figs. 12 and 13 (ρ_2 is radius of receiver crystal). Fig. 12 applies to the usual case of two crystals of the same size, or one crystal and a plane reflector. For Fig. 13 the radius of the receiver crystal is $\frac{1}{3}$ that of the transmitter. The curve shows an oscilla-

tory motion at small separation and a pronounced maximum near $d = 1.2\rho_1^2/\lambda$, at which point presumably it is being effectively irradiated by all parts of the transmitter crystal. The value of the average pressure here is nearly 60 per cent. greater than the value, P, at the transmitter.

Case II: The Radiation Pattern in a Semi-Infinite Tube with a Vibrating Crystal at One End.

The analysis of ultrasonic propagation in a tube of semi-infinite length depends on the choice of boundary conditions at the wall of the tube which correspond to physical reality. If the boundary condition taken is that the normal component of the velocity at the wall of the tube shall be zero, then for a system with a transmitter equal to the tube radius a nearly plane wave can be made to travel down the tube.

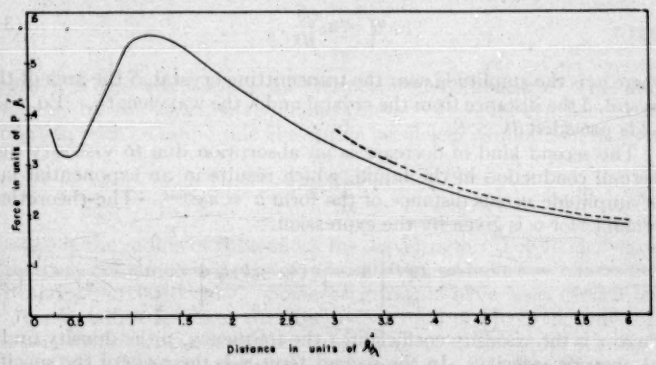

FIG. 13. Force on receiver crystal ($\rho_2 = \frac{1}{3}\rho_1$) vs. distance between crystals. The radius of the receiving crystal is one-third of the transmitter.

If the radius of the transmitter is less than the radius of the tube, the disturbance in the tube can be considered as the sum of the disturbances due to an infinite number of cylindrical modes travelling down the tube with differing velocities.

Another boundary condition which may be reasonable in some cases is that the pressure at the wall of the tube is zero. Such a boundary condition may be approximately valid when there are air spaces between the fluid and the tube (as often occur for mercury in a steel tube). With this boundary condition it is found that a series of cylindrical modes will travel down the tube with varying velocities. We are indebted to Mr. H. J. McSkimin of the Bell Telephone Laboratories for allowing us to see his unpublished analysis of this situation. His results show that the intensity of the ultrasonic beam falls off very

slightly at large distances in the tube in contrast to the inverse square law spreading of the free-space beam.

In Section D where viscosity effects also are considered there will be presented some experimental data on the question of propagation of waves in tubes.

D. ATTENUATION.

Free Space Beam

A "free space" beam in a liquid decreases in two distinct ways. There is first the spreading of the beam due to diffraction, which gives rise to an inverse square law for the intensity as large distances from the transmitting crystal (see eq. 28b of preceding section). The amplitude behavior can be described by

$$a = a_0 \frac{S}{d\lambda}, \tag{31}$$

where a_0 is the amplitude near the transmitting crystal, S the area of the crystal, d the distance from the crystal and λ the wavelength. Eq. (31) holds provided $d\lambda > S$.

The second kind of decrease is an absorption due to viscosity and thermal conduction in the liquid, which results in an exponential law for amplitude versus distance of the form $a = a_0 e^{-\alpha d}$. The theoretical formula [8] for α is given by the expression.

$$\alpha = \frac{2\eta^2 f^2}{\rho v^3}\left[\frac{4}{3}\eta + \frac{(\gamma - 1)K}{c_p}\right], \tag{32}$$

where η is the viscosity coefficient, f the frequency, ρ the density and v the acoustic velocity. In the second term γ is the ratio of the specific heats, K the thermal conductivity and c_p the specific heat at constant pressure. For non-metallic liquids the effect of thermal conduction is negligible. For many liquids this simple theory predicts an attenuation much smaller than that found by experiment. For mercury, however, which was widely used in delay line operation, agreement is good. Theory predicts an attenuation of about 1.1 db. per ft. at 10 mc., whereas the experimental values indicate 1.2 ± .2 db. per ft. Here the heat conduction loss accounts for 80 per cent. of the attenuation.

Since the viscosity coefficient decreases with rising temperature, attenuation generally decreases also. The effect is very marked in the case of water.[9]

[8] W. P. Mason, "Electromechanical Transducers and Wave Filters," Van Nostrand, p. 305 (1942).

[9] C. E. Teeter, Jr., *J. Acous. Soc. Am.*, **18**, 488 (1946).

Guided Beam

It seems to be possible to avoid at least in part the decrease due to spreading of the beam by confining the beam within a tube of the same diameter as the transmitting crystal. This is what is meant by a guided beam. If the liquid could slip freely over the tube surface, a piston-like motion would take place corresponding to perfect plane-wave propagation, without any loss due to spreading. Actually, the conditions at the wall are not as simple as this and depend on the nature of the surface. A possible assumption is that the liquid sticks to the surface instead of sliding freely over it. Crandall [10] has shown that the viscous losses take place in a very thin layer, of the order of 10^{-6} cm. in thickness, across which a major portion of the velocity change occurs. The thickness of the layer is given by

$$\delta = \left(\frac{\eta}{\pi\rho f}\right)^{\frac{1}{2}}, \tag{33}$$

where η is the viscosity, ρ the density, f the frequency. The drag produced by the layer on the liquid column causes an exponential attenuation with an amplitude absorption coefficient per unit length given by

$$\beta = \frac{2\pi\delta}{b\lambda}, \tag{34}$$

where b is the radius of tube and λ the wavelength. For 10 mc. waves in mercury contained in a tube of radius 0.3 cm. we have $\delta = 2.85 \times 10^{-6}$ cm. and $\beta = 0.0040$ cm^{-1}. Some experiments have been carried out at 10 mc. which indicate that the attenuation of ultrasonic waves in mercury shows a dependence on tube diameter of this order of magnitude. The effect was, however, influenced by the character of the tube's inner surface. It has already been mentioned in Section C that the boundary conditions may have a profound effect. For example, if, instead of a high acoustic impedance in the steel wall, the air occluded in the irregularities of wall surface offers a low impedance, there will be no energy absorption at the tube wall and the propagation will always consist of many cylindrical waves travelling with different velocities down the tube.

Since the guided beam is not subject to the attenuation from spreading given by equation (31), total attenuation is generally less in this case than for the free space beam. Only for long distances can the tubular attenuation give an effect comparable with the spreading. Of course both beams are subject to the absorption varying as the square of the frequency (eq. 32).

[10] I. B. Crandall, "Theory of Vibrating Systems and Sound," Van Nostrand, p. 229 (1927).

Science Captures a Chinese Art.—In China the making of soya sauce is mainly a household art, with grandmothers passing along to daughters and granddaughters the details of recipes and the strains of ferments used in the process.

In the United States, soya sauce—as is true of many other food products—is chiefly a factory product. Each manufacturer is concerned not only with producing a sauce of high quality, but also a standardized sauce in which each batch will have the flavor, color, and taste of every other batch. This calls for standardization of the raw materials and for use of standard strains of microorganisms in the fermentation of the sauce.

The U. S. Department of Agriculture has announced that strains of four organisms desirable in preparing soya sauce have been added to the culture collection of industrial ferments at the Northern Regional Research Laboratory at Peoria, Ill. These include two molds, a yeast, and a bacterium. They will be maintained as pure cultures and will be available to industrial users. This makes it possible for a fermenter to make a fresh start with new and pure cultures, if at any time his stock cultures become contaminated with "wild" molds or yeasts that injure the quality or uniformity of his product.

The Fermentation Division of the Bureau of Agricultural and Industrial Chemistry credits Mr. Pei Sung King of the National Bureau of Industrial Research, Chungking, China, with aid in selecting the strains of organisms and standardizing a process of fermentation that yields a high-quality sauce. Mr. King has been a guest worker at the Northern Laboratory, and suggested various methods of fermentation which the scientists tested and compared in working out the method they now recommend to manufacturers. It is not practical for home use or for small quantities of sauce.

The preparation of soya sauce calls for a brine fermentation of the beans for from 30 to 90 days. But the "starter" used in this process is a mixture of three previously prepared cultures; (1) of a mold that develops on cooked rice; (2) of a yeast working on soya broth; and (3) of a bacterial fermentation of soya broth. For a quality product these should be mixed at the right stage of development in suitable proportions.

R. H. O.

AN INTEGRAL-EQUATION APPROACH TO PROBLEMS OF VIBRATING BEAMS.*

BY

WALTER T. WHITE, Sc.D.†

PART I.

ABSTRACT.

In this paper integral equations are applied for the calculation of the normal modes of vibrating beams. Both exact and approximate methods of solving the integral equation are considered. The Green's function, or kernel, of the integral equation is constructed for both uniform and nonuniform beams. Solutions for the normal modes of a uniform cantilever are given. A nonuniform, naturally-twisted turbine blade is studied in detail and the first and second normal modes are calculated by the integral-equation method.

1. INTRODUCTION.

In many mechanical designs, it is important to eliminate vibrations associated with mechanical resonance. Calculations of the normal modes of the system often reveal objectionable resonances, and when they are known, methods can be devised to reduce or eliminate them. In some cases, damping or appropriate shock mounting may achieve the desired result. But in others, it is necessary to change the inertia and stiffness of the system. The theory of vibrating beams, when applicable, is the most effective basis for such calculations.

Vibrating members treated as beams are rotating shafts, turbine blades, hulls of ships, airplanes, missiles, and other complex structures. The beam and its supports may be sufficiently simple for straightforward analysis by classical methods with differential equations. If the problem is complicated by variations of physical properties, the solution by integral equations gives results more conveniently than solution by differential equations. The formulation of an integral equation is based upon a simple picture of the beam and the application of the superposition principle. Variations of physical properties and such effects as rotary inertia, longitudinal inertia, and gyroscopic moment cause no particular difficulty with the integral-equation formulation.

The purpose of this paper is to outline the integral-equation approach to the calculation of normal modes of vibrating beams. Certain properties of integral equations required for the solution of practical problems are given. A method is developed for constructing the kernels for the integral equations of vibrating beams. To demonstrate the integral-equation method and its accuracy, an application is made to a

* This paper is from a thesis, "Integral-Equation and Approximate Solutions for Normal Modes of Vibration," submitted to the department of Electrical Engineering, M.I.T., 1941.

† Research Engineer, Sperry Gyroscope Co., Great Neck, N. Y.

simple cantilever. A second application is made to a nonuniform naturally-twisted turbine blade.

2. FORMULATION OF THE INTEGRAL EQUATION.

Two procedures generally are available for the integral-equation formulation of a vibration problem: (1) obtain the differential equation, and then make a transformation to the integral equation; (2) formulate the integral equation directly from the physical nature of the problem. Evidently the second procedure has distinct advantages. Indeed, one of the principal advantages of the integral-equation treatment is the closeness with which it is tied in with the physical picture.

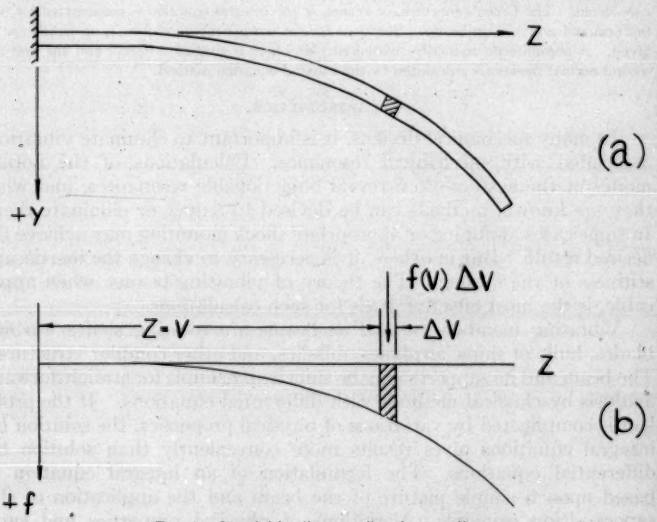

FIG. 1. Inertial loading on vibrating cantilever.

As an example, consider the cantilever. To formulate the integral equation, it is necessary to consider the inertial loading while the cantilever is freely vibrating. If the cantilever is observed at the instant of its maximum downward deflection, as in Fig. 1a, each elemental mass has a deflection $+y(z, t)$ and an upward acceleration $-a(z, t)$. The product of mass m per unit length and acceleration gives the upward inertial force which the beam exerts upon its mass. By the principle of action and reaction, the mass exerts a downward force or loading $f(z, t)$ per unit length that is given by

$$f(z, t) = -ma(z, t). \tag{1}$$

The loading on an elemental length Δv is equivalent to a concentrated load $f(v)\Delta v$ (see Fig. 1b). From texts on strength of materials,*,[1] the static deflection of a uniform cantilever caused by a unit-concentrated load applied at $z = v$ is

$$\left.\begin{aligned} G(z, v) &= z^2(3v - z)/6EI, \qquad z \leq v \\ &= v^2(3z - v)/6EI, \qquad v \leq z \end{aligned}\right\}, \tag{2}$$

where EI is the flexural rigidity of the cantilever. The static deflection caused by a unit-concentrated load generally is called a *Green's function*. The deflection caused by the loading $f\Delta v$ is

$$\Delta y(z, v) = G(z, v)f(v)\Delta v. \tag{3}$$

By superposition, the deflection at z is given as the summation of the deflections caused by each elemental loading along the beam, or

$$y(z, t) = \int_0^L G(z, v)f(v, t)dv. \tag{4}$$

The time variable t is introduced, since the loading f in Eq. 1 is a time-varying quantity.

Since undamped oscillations of small amplitude are harmonic functions of time, $y(z, t)$ can be written as

$$y(z, t) = y(z) \sin \omega t, \tag{5}$$

where ω is the frequency of oscillation in radians per second. The acceleration is obtained by differentiation of Eq. 5, and is

$$a(z, t) = -\omega^2 y(z) \sin \omega t. \tag{6}$$

Substitutions from Eqs. 1, 5 and 6 in Eq. 4 gives

$$y(z) \sin \omega t = m\omega^2 \int_0^L G(z, v)y(v) \sin \omega t dv. \tag{7}$$

Since the time function is not dependent upon the variable of integration, it is cancelled to give

$$y(z) = \lambda \int_0^L G(z, v)y(v)dv, \tag{7a}$$

where the constants are lumped in the parameter λ.

Equation 7a is the *integral equation* for the freely vibrating cantilever. The *kernel*, or Green's function, $G(z, v)$, is given by Eq. 2, and y and λ are unknowns. The problem is to find values of λ for which non-zero functions y exist. Equation 7a is called a *homogeneous integral equation;* the λ's are called *eigenvalues* and the corresponding y's are called *eigenfunctions*. The eigenvalues and eigenfunctions determine the *normal modes* of vibration for the cantilever.

* For numbered references see Bibliography.

3. PROPERTIES OF HOMOGENEOUS INTEGRAL EQUATIONS.

Before completing the solution of Eq. 7a for the cantilever, it is well to consider certain properties of homogeneous integral equations[2, 3] which are useful in the solution of practical problems.

A general form of the homogeneous integral equation is

$$y(z) = \lambda \int_a^b K(z, v)y(v)dv, \tag{8}$$

where a and b are constants and $K(z, v)$ is the kernel corresponding to the Green's function in Eq. 7a. In vibrations and related problems, the kernel is often a symmetric function of z and v:

$$K(z, v) = K(v, z). \tag{9}$$

If the kernel is asymmetric, it can be made symmetric by a simple transformation, as will be shown later. In practical problems the kernel is real, continuous and not zero on the interval (a, b).

An obvious solution of Eq. 8 is

$$y(z) = 0.$$

Although this result yields no useful information, useful solutions can be found. For certain eigenvalues λ there exist corresponding solutions or eigenfunctions y which are written

$$\left.\begin{aligned} y_1(z) &= \lambda_1 \int_a^b K(z, v)y_1(v)dv \\ y_2(z) &= \lambda_2 \int_a^b K(z, v)y_2(v)dv \\ &\cdots\cdots\cdots \\ y_n(z) &= \lambda_n \int_a^b K(z, v)y_n(v)dv \\ &\cdots\cdots\cdots \end{aligned}\right\} \tag{10}$$

Clearly, each eigenfunction is determined only within a constant multiplying factor, for, if $y_n(z)$ is a solution of Eq. 8, substitution shows that $cy_n(z)$ is a solution where c is a constant. Solutions in Eqs. 10, therefore, only determine the form of the eigenfunctions. The eigenvalues, however, are uniquely determined.

A general property for eigenfunctions of symmetric kernels is their orthogonality. This property is expressed as

$$\int_a^b y_m(v)y_n(v)dv = 0, \qquad (m \neq n). \tag{11}$$

If $m = n$, the integral has a value N_n called the *norm*; that is,

$$\int_a^b [y_n(v)]^2 dv = N_n. \tag{12}$$

A useful property of the kernel is its *bilinear expansion*. For an infinity of eigenvalues and eigenfunctions, the bilinear expansion is given as

$$K(z, v) = \sum_{n=1}^{\infty} y_n(z) y_n(v)/\lambda_n N_n. \tag{13}$$

This series expansion for the kernel must be uniformly convergent for all values of z and v on the interval (a, b). The expansion is Hilbert's bilinear formula.[2] It gives the kernel in the manner of a Fourier series in terms of the eigenfunctions. When applied to physical problems the uniform convergence is assured.

Often the kernel is asymmetric. For example, if the cantilever which led to Eq. 7a has a nonuniform cross section and loading, there is associated with the Green's function a function $\mu(v)$ which takes care of the variations of mass and flexural rigidity along the length of the cantilever. The integral equation then has the form

$$y(z) = \lambda \int_0^L G(z, v)\mu(v) y(v) dv, \tag{14}$$

and the kernel is

$$K(z, v) = G(z, v)\mu(v). \tag{15}$$

Obviously, the kernel is asymmetric, since

$$K(z, v) \neq K(v, z).$$

By a simple transformation, the asymmetric kernel can be made symmetric. Multiply Eq. 14 by $\sqrt{\mu(z)}$ and define a new eigenfunction

$$Y(z) = y(z)\sqrt{\mu(z)}, \tag{16}$$

and a new kernel

$$K_s(z, v) = G(z, v)\sqrt{\mu(z)\mu(v)}. \tag{17}$$

With these substitutions Eq. 14 is written

$$Y(z) = \lambda \int_0^L K_s(z, v) Y(v) dv. \tag{18}$$

Since the kernel of Eq. 17 is symmetric, Eq. 18 can be treated as an integral equation with a symmetric kernel. The orthogonality condition from Eqs. 11 and 16 is

$$\int_0^L \mu(v) y_m(v) y_n(v) dv = 0, \qquad (m \neq n). \tag{19}$$

The foregoing properties are useful for the solution of practical integral equations. However, complex kernels arise in certain problems and such problems require special orthogonality conditions and a more complicated bilinear expansion. After the formulation of the problem, an inspection will reveal whether the integral equation is similar to Eq. 8 or 14, or whether it is more complex and requires the derivation of a special orthogonality condition or bilinear expansion.

4. SOLUTION OF INTEGRAL EQUATIONS.

Practical methods for solving integral equations seldom are exact. More often solutions are obtained by approximations, and with reasonable effort such solutions can be calculated with an accuracy comparable to the physical data. Two methods frequently used for solving integral equations are:

1) Obtain a solution by an intuitive guess, and prove it by substitution.
2) Obtain a solution by *successive approximations*.

As an example of solution by the first method, consider the cantilever of Eq. 7a. Substitution of the Green's function from Eq. 2 gives

$$y(z) = \lambda \int_0^z v^2(3z - v)y(v)dv + \lambda \int_z^L z^2(3v - z)y(v)dv,$$

where

$$\lambda = m\omega^2/6EI.$$

As a guess for the solution, try the equation

$$y(z) = B \cosh kz + C \sinh kz + D \cos kz + E \sin kz.$$

Substitution in the integral equation gives the eigenvalue

$$\lambda = k^4/6,$$

and the eigenfunction

$$y(z) = \cosh kz - \cos kz + b\,(\sinh kz - \sin kz).$$

The constant b is

$$\left.\begin{aligned} b &= -(\sinh kL - \sin kL)/(\cosh kL + \cos kL) \\ &= -(\cosh kL + \cos kL)/(\sinh kL + \sin kL) \end{aligned}\right\},$$

where kL is a root of

$$\cosh kL \cos kL + 1 = 0.$$

A few values of kL are

$$\begin{aligned} k_1L &= 1.8751, \\ k_2L &= 4.6941, \\ k_3L &= 7.8548. \end{aligned}$$

From the foregoing the first three natural frequencies of the canti-

lever are obtained from the eigenvalues as

$$\omega_1 = (3.516/L^2)\sqrt{EI/m},$$
$$\omega_2 = (22.03/L^2)\sqrt{EI/m},$$
$$\omega_3 = (61.70/L^2)\sqrt{EI/m} \text{ radians per second.}$$

Generally, a guess as in the foregoing will not lead to the solution in a closed form. One reason for this is that the Green's function may be known only as a family of curves. For problems not easily solved in closed form, the method of successive approximations is appropriate. When used with numerical or machine integration, the method of successive approximations is applicable to problems in which the kernel is known from tabulated data or plotted curves.

In the method of successive approximations, the normal modes are calculated singly beginning with the first, or lowest mode, and continuing in order to the higher modes. For the first mode, an approximation to the eigenfunction is used as a *generating function*. It is necessary only that the generating function be *not orthogonal* to the first eigenfunction. Although it is improbable that a function arbitrarily selected would be orthogonal to the unknown eigenfunction, it can be shown that a Green's function is certain of meeting the non-orthogonality condition. Accordingly, the generating function $g_0(z)$ is taken as

$$g_0(z) = G(z, a), \tag{20}$$

where a is an arbitrary value which gives a Green's function not identically zero.

For the first eigenfunction, select for a the value where judgment indicates a concentrated load to be most nearly equivalent to the distributed inertial load. For the uniform cantilever the value is approximately $a = 0.8L$. (The best value can be shown to be $a = 0.8021L$.) When the generating function is selected by this method, solutions are obtained with a small number of successive approximations. Therefore, unless some other function obviously has advantages, a Green's function is used as the generating function.

From the generating function $g_0(z)$, a set of equations is formed by successive iterations with the kernel. For the cantilever the iterations follow from Eq. 14 as

$$\left.\begin{aligned} g_1(z) &= \int_0^L G(z, v)\mu(v)g_0(v)dv \\ g_2(z) &= \int_0^L G(z, v)\mu(v)g_1(v)dv \\ &\cdots\cdots\cdots\cdots \\ g_{n+1}(z) &= \int_0^L G(z, v)\mu(v)g_n(v)dv \end{aligned}\right\} \tag{21}$$

As n becomes large, these successive iterations give the solution of the integral equation [3] as

$$y_1(z) = g_n(z). \tag{22}$$

This is the eigenfunction of the first mode. The first eigenvalue is calculated by substitution of Eq. 22 in Eq. 14 which gives

$$g_n(z) = \lambda_1 \int_0^L G(z, v)\mu(v)g_n(v)dv. \tag{23}$$

Substitution from Eqs. 21 gives

$$g_n(z) = \lambda_1 g_{n+1}(z). \tag{23a}$$

The eigenvalue λ_1 is calculated from Eq. 23a for any value of z. However, where approximate methods are used, a more accurate value of λ_1 is calculated as the average value

$$\lambda_1 = \frac{\int_0^L g_n(v)dv}{\int_0^L g_{n+1}(v)dv}. \tag{24}$$

Usually the first eigenvalue is calculated after one to three iterations. The first eigenfunction generally is calculated after two to four iterations. Since the convergence is very rapid, the calculation of the eigenfunction is complete when the form of $g_{n+1}(z)$ is similar to $g_n(z)$.

Calculation of the second eigenvalue and eigenfunction by approximate methods is possible only after calculation of the first eigenfunction. A generating function is selected which is orthogonal to the first eigenfunction and not orthogonal to the second eigenfunction. The first condition is met by a procedure to be developed below. As for the second condition, it is improbable that an arbibrary function would be orthogonal to the unknown eigenfunction; yet, where certainty is desired, a Green's function given by Eq. 20 is selected. A good value to choose for a is the estimated coordinate where the maximum deflection of the beam occurs when it is vibrating in the second mode.

To construct a generating function $g_0(z)$ orthogonal to the first eigenfunction $y_1(z)$, form the equation [4]

$$g_0(z) = f_0(z) - \alpha y_1(z), \tag{25}$$

where α is a constant and $f_0(z)$ is an arbitrary function, preferably a Green's function $G(z, a)$. Multiplication of Eq. 25 by $\mu(z)y_1(z)$ and integration over the length of the beam give

$$\int_0^L \mu(z)y_1(z)g_0(z)dz = \int_0^L \mu(z)y_1(z)f_0(z)dz - \alpha \int_0^L \mu(z)y_1^2(z)dz. \tag{26}$$

The integral on the left is the required orthogonality condition and is

zero if

$$\alpha = \frac{\int_0^L \mu(z) y_1(z) f_0(z) dz}{\int_0^L \mu(z) y_1^2(z) dz}. \tag{27}$$

Accordingly, the generating function for the second eigenfunction can be constructed from Eq. 25 with α evaluated by Eq. 27.

Successive iterations of the generating function for the second eigenfunction give

$$\left.\begin{aligned} g_1(z) &= \int_0^L G(z, v)\mu(v) g_0(v) dv \\ &\cdots\cdots\cdots\cdots \\ g_{n+1}(z) &= \int_0^L G(z, v)\mu(v) g_n(v) dv \end{aligned}\right\}. \tag{28}$$

If each integration is *exact*, the nth iteration approaches the second eigenfunction as n becomes large. However, exactness is possible only with formal integration, and if approximate integration is used, a special procedure is required to assure the convergence of Eqs. 28 to the second eigenfunction. The procedure simply is to make certain that each successive generating function is orthogonal to the first eigenfunction. This requires a construction similar to Eq. 25 after each iteration to obtain an orthogonalized generating function, $g'_n(z)$, given by

$$g'_n(z) = g_n(z) - \alpha_n y_1(z). \tag{29}$$

The $(n + 1)$ iteration gives

$$g_{n+1}(z) = \int_0^L G(z, v)\mu(v) g'_n(v) dv. \tag{30}$$

As n becomes large, the second eigenfunction is the orthogonalized $g'_{n+1}(z)$ and is given by

$$y_2(z) = g_{n+1}(z) - \alpha_{n+1} y_1(z). \tag{31}$$

The second eigenvalue is given by a relation similar to Eq. 24 as

$$\lambda_2 = \frac{\int_0^L g'_n(v) dv}{\int_0^L g'_{n+1}(v) dv}. \tag{32}$$

Another method for calculation of the second eigenfunction makes use of the bilinear expansion, Eq. 13. Since Eq. 13 is for a symmetric kernel, the integral equation must be in the form of Eq. 18:

$$Y(z) = \lambda \int_0^L K_s(z, v) Y(v) dv. \tag{18}$$

The bilinear formula gives

$$K_s(z, v) = \sum_{n=1}^{\infty} Y_n(z) Y_n(v)/\lambda_n N_n. \tag{13a}$$

If the first eigenfunction and eigenvalue are known, they are subtracted from $K_s(z, v)$ to give the *perturbated kernel* $K_p(z, v)$,

$$K_p(z, v) = K_s(z, v) - Y_1(z) Y_1(v)/\lambda_1 N_1. \tag{33}$$

Since the remaining eigenfunction components in $K_p(z, v)$ are orthogonal to $Y_1(z)$, no error results in the calculation of the second eigenfunction if the pertrubated kernel, $K_p(z, v)$, is used instead of $K_s(z, v)$. Hence, with a suitable generating function, which need not be orthogonal to the first eigenfunction, the second eigenfunction is calculated by successive iterations to give

$$\left.\begin{aligned} g_1(z) &= \int_0^L K_p(z, v) g_0(v) dv \\ &\cdots\cdots\cdots\cdots \\ g_{n+1}(z) &= \int_0^L K_p(z, v) g_n(v) dv \end{aligned}\right\}. \tag{34}$$

There is no tendency to converge to the first eigenfunction and successive generating functions are not required to be made orthogonal to the first eigenfunction. For large values of n the second eigenfunction is given by

$$Y_2(z) = g_n(z), \tag{35}$$

and the second eigenvalue is

$$\lambda_2 = \frac{\int_0^L g_n(v) dv}{\int_0^L g_{n+1}(v) dv}. \tag{36}$$

The extension of the foregoing method to the calculation of higher modes is straightforward. A new perturbated kernel is formed by subtraction of previously calculated components from the bilinear formula, and the next higher mode is calculated by relations similar to Eqs. 34, 35 and 36. Alternatively, the higher modes are calculated as in Eqs. 28 and 29 provided the generating function for each successive iteration is made orthogonal to the previously calculated lower modes.

An application of the foregoing methods is made for the calculation of the first two normal modes of the uniform cantilever. Although the complete solution was obtained for the integral equation, the method of successive approximations is used for purposes of illustration. A comparison of numerical results from the approximate method with the exact solution illustrates the accuracy of the method.

Several means are available for the numerical evaluation of the integrals. A standard calculating machine can be used with Simpson's rule. Machines, such as the cinema integraph [5] or the differential analyzer,[6] if available, can be used for evaluation of the integrals. In this example the differential analyzer is used.

The integral equation to be solved is

$$y(z) = \lambda \int_0^L K(z, v)y(v)dv,$$

where $K(z, v)$ is a symmetric kernel and is obtained from Eq. 2 as

$$\left.\begin{aligned} K(z, v) &= z^2(3v - z), \quad z \leq v \\ &= v^2(3z - v), \quad v \leq z \end{aligned}\right\}.$$

λ is the eigenvalue which includes the unknown natural frequency and the constants of the equation. In this example

$$\lambda = m\omega^2/6EI.$$

If the integral equation is non-dimensionalized by the substitutions

$$\left.\begin{aligned} z &= z'L \\ v &= v'L \end{aligned}\right\},$$

it is written in non-dimensional form (with the primes omitted for convenience) as

$$y(z) = \lambda \int_0^1 K(z, v)y(v)dv,$$

and

$$\lambda = mL^4\omega^2/6EI.$$

Numerical values for the kernel of the integral equation are in Table I. From the estimated form of the freely vibrating cantilever, the generat-

TABLE I.

Symmetric Kernel for Uniform Cantilever.

$K(z, v) = z^2(3v - z), z \leq v, K(z, v) = K(v, z)$

(Multiply by 10^{-3})

z / v	0.0	0.1	0.2	0.3	0.4	0.5	0.6	0.7	0.8	0.9	1.0
0.0	0										
0.1	0	2									
0.2	0	5	16								
0.3	0	8	28	54							
0.4	0	11	40	81	128						
0.5	0	14	52	108	176	250					
0.6	0	17	64	135	224	325	432				
0.7	0	20	76	162	272	400	540	686			
0.8	0	23	88	189	320	475	648	833	1024		
0.9	0	26	100	216	368	550	756	980	1216	1458	
1.0	0	29	112	243	416	625	864	1127	1408	1701	2000

ing function is taken as

$$g_0(z) = kz^2,$$

where k is any convenient constant. Two successive iterations of the generating function, as in Eqs. 21, are sufficient to evaluate the eigenfunction. The results from the second iteration are in Table II, as are the exact values. The eigenvalue is calculated from Eq. 24, and the natural frequency, calculated from the eigenvalue, is given in Table II. The errors between the exact and calculated values for both the eigenfunction and natural frequency are negligible. The normalization constant is calculated from Eq. 12 and listed in Table II.

For the evaluation of the second mode, the perturbated kernel is calculated from Eq. 33 as

$$K_p(z, v) = z^2(3v - z) - y_1(z)y_1(v)/\lambda_1 N_1, \qquad z \leq v.$$

The values of $y_1(z)$, λ_1 and N_1 tabulated in Table II for the second

TABLE II.

Normal Modes of Uniform Cantilever.

z	$y_1(z)$: First Mode		$y_2(z)$: Second Mode	
	Exact	Second Iteration	Exact	Third Iteration
0.0	0.0000	0.0000	0.000	0.000
0.1	0.0168	0.0168	−0.092	−0.092
0.2	0.0639	0.0639	−0.301	−0.300
0.3	0.1365	0.1366	−0.526	−0.525
0.4	0.2299	0.2302	−0.683	−0.685
0.5	0.3395	0.3391	−0.714	−0.721
0.6	0.4611	0.4612	−0.589	−0.600
0.7	0.5908	0.5905	−0.317	−0.323
0.8	0.7255	0.7247	0.070	0.075
0.9	0.8624	0.8635	0.524	0.509
1.0	1.0000	0.9997	1.000	0.986
ω: Natural frequency in radians per second				
	$\frac{3.5160\sqrt{EI/m}}{L^2}$	$\frac{3.5176\sqrt{EI/m}}{L^2}$	$\frac{22.03\sqrt{EI/m}}{L^2}$	$\frac{22.04\sqrt{EI/m}}{L^2}$
N: Normalization constant				
	2.001	2.001		

iteration are used for calculation of $K_p(z, v)$. The generating function for the second mode is

$$g_0(z) = kK_p(z, 0.6),$$

where k is a convenient constant multiplier. The results from the third iteration of the generating function are compared with the exact values in Table II. The errors for the approximate calculation of the second mode are almost as small as the errors for the first mode.

(To be continued in next issue.)

VISUAL MEASUREMENTS OF SHORT PULSES OF DIRECT CURRENT.

BY

PHILIP F. ORDUNG.*†

Yale University,
1946.

SYNOPSIS.

Within recent years, engineering applications using pulses of direct current as short in duration as a microsecond and repeated several thousand times per second have become important. Such pulses may have amplitudes that are greater than 100 amperes. This paper discusses the techniques and precautions which are essential for oscillographic observations of such pulses. Particular consideration is given to the problem of determination of the bandwidths required for measurements of such pulses, of the construction and the calibration of resistors for metering such currents, and of properly terminating the coaxial transmission line used for connecting the metering element to the oscillograph.

INTRODUCTION.

With the advances and developments of recent years in the application of electron tubes has come an increasing need for accurate measurements of short pulses of direct current. The information which must be supplied by the measurements is the shape, amplitude, duration, and repetition rate of the pulse. Methods have been developed using meters for measuring the amplitude and the repetition rate of the pulse. However, visual observation of the pulse by means of an oscillograph is the only method which can give accurate data concerning the shape and the duration of the pulse. The general arrangement of the components for the oscillographic method with which this paper is concerned is shown in Fig. 1. The pulse current, shown as "i" on the figure, flows through the metering element. The corresponding voltage pulse developed across the metering element is transmitted to and viewed on the oscillograph. For this type of measurement, the sweep of the oscillograph must be synchronized to the pulse being viewed and the interval of duration of the sweep trace must be slightly greater than that of the pulse.

The types of pulses that may be encountered in the applications of pulse techniques are of a great variety. Typical pulses of current have intervals of duration between a fraction of microsecond and several hundred microseconds and have amplitudes ranging from several amperes to greater than one hundred amperes. One such pulse is shown in Fig. 5A. The shape of such pulses is approximately trapezoidal with

* Assistant Professor Yale School of Engineering, Yale University, New Haven, Connecticut.

† Formerly with the Naval Research Laboratory where this work was begun.

periods of rise and decay that are short in comparison to the pulse-duration. The repetition rates for these pulses range from several pulses per second to several thousand pulses per second. The problem of measuring such widely differing pulses is great, but the precautions which must be observed in their measurement are similar.

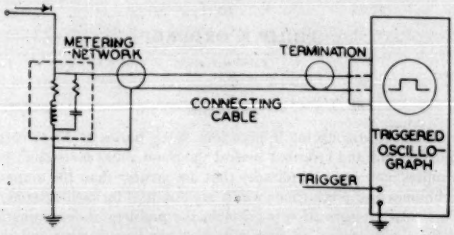

FIG. 1. Circuit for visual measurement of repeated pulses of current.

BANDWIDTH FOR PULSE MEASUREMENTS.

The measuring equipment in order to faithfully reproduce the shape of a repeated pulse must represent all of the frequency components contained in the pulse. For the purpose of determining the necessary bandwith for representing the pulse, Fourier Analysis is applied to the repeated square pulse shown in Fig. 2. T_R is the period of the pulse,

V.2
194

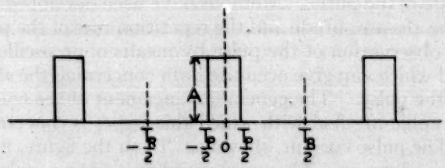

FIG. 2. Wave of repeated square pulses of amplitude, A, period, T_R, and pulse width T_P.

and T_P is the duration of the pulse. In functional form, the shape of one cycle of this pulse wave may be represented as follows:

$$f(t) = A \qquad -\frac{T_P}{2} \leq t \leq \frac{T_P}{2}$$

$$f(t) = 0 \qquad -\frac{T_R}{2} < t < -\frac{T_P}{2} \qquad \frac{T_P}{2} < t < \frac{T_R}{2}. \qquad (1)$$

By conventional Fourier Analysis, the pulse wave may be represented as

$$f(t) = \tfrac{1}{2}a_0 + \sum_{k=1}^{\infty} a_k \operatorname{Cos} \frac{2\pi k t}{T_R}, \qquad k = 1, 2, 3, 4 \cdots \qquad (2)$$

where

$$a_k = \frac{2}{T_R}\int_{-T_R/2}^{T_R/2} f(t)\,\mathrm{Cos}\,\frac{2\pi kt}{T_R}\,dt. \qquad (2A)$$

The amplitudes of the frequencies required to represent the pulse are determined by substituting the functional form of the pulse, Eq. (1), into Eq. (2A). For the case of the repeated pulse being discussed, the Fourier series representation is

$$f(t) = A\,\frac{T_P}{T_R} + \sum_{k=1}^{\infty}\frac{2A}{\pi k}\,\mathrm{Sin}\,\pi k\,\frac{T_P}{T_R}\,\mathrm{Cos}\,\frac{2\pi kt}{T_R}. \qquad (3)$$

The angular frequency components contained in the repeated pulse are given in this series by the term $2\pi k/T_R$, where k is the order of the harmonic of the repetition frequency F_R. Using Eq. (3), the frequency spectrum shown in Fig. 3 is plotted. The envelope of the spectrum is

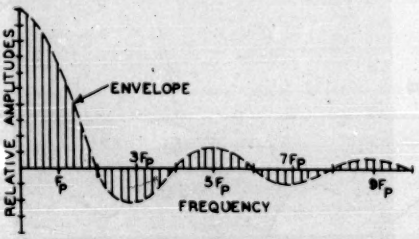

FIG. 3. Frequency spectrum corresponding to a repeated pulse wave in which $T_R = 10T_P$ and $F_P = 5F_R$.

shown by the dashed lines. Significant points in the envelope occur at frequencies that correspond to values of k such that

$$2kT_P/T_R = m. \qquad m = 1, 2, 3, 4, 5 \cdots \text{etc.} \qquad (4)$$

Since the term $2\pi k/T_R$ in Equation (3) expresses angular frequency, k/T_R is frequency. The particular value of this frequency, k/T_R, that is obtained when $m = 1$, is defined to be the pulse-width frequency F_P and has a period twice that of the pulse width, $F_P = 1/2T_P$. For the even integer values of m, the magnitude of the envelope is zero. For the odd harmonics of the pulse-width frequency (frequencies that correspond to the odd integer values of m), the amplitudes of the minor lobes of the spectral envelope are approximately maximum. Thus, changing the repetition rate of a repeated pulse has no effect on the shape of the envelope of the frequency spectrum; however the number of frequencies represented in each lobe of the envelope is changed.

For a square wave, $T_P = T_R/2$, the frequencies representing the pulse are odd harmonics of the pulse-width frequency. When the pulse-

width frequency is a multiple of the repetition frequency (T_R/T_P an integer), the spectrum includes the frequencies required to represent a square wave with the given pulse width and additional frequencies located symmetrically in each lobe of the spectral envelope about the square-wave frequencies. The additional frequencies eliminate the pulses in the square wave that are not contained in the wave having the reduced repetition rate. This suggests that the number of lobes in the envelope of the frequency spectrum required to approximate a pulse of given width to a desired accuracy is the same for a square wave and for repetition rates that are submultiples of the pulse-width frequency. Generalized, this argument extends to all repetition rates less than the pulse-width frequency provided that the pulse separation is such that $\omega_1(T_R - T_P) > 18$. (See the Appendix.)

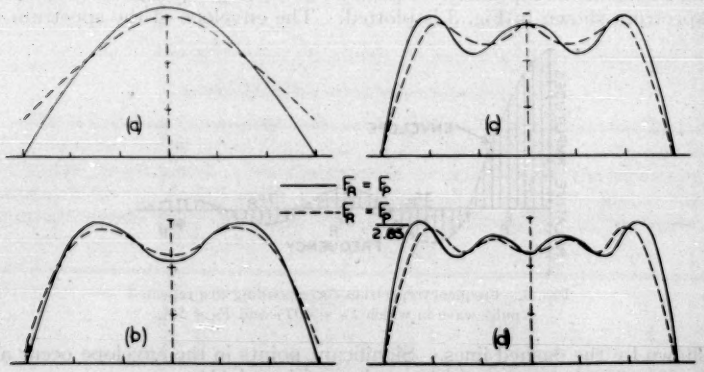

FIG. 4. Approximations to a square pulse of given width for two repetition rates—$F_R = F_P$, and $F_R = F_P/2.85$. The maximum frequencies included in the pass band for the approximations are as follows: (a) $2F_P$; (b) $4F_P$; (c) $6F_P$; and (d) $8F_P$.

Approximations of a given square pulse for two repetition rates, one of which is that for a square wave, are shown in Fig. 4. For both repetition rates, the inclusion of all frequencies to the eighth harmonic of the pulse-width frequency gives similar trapezoidal approximations having rise and decay periods less than 12 per cent. of the duration of the pulse and having less than 12 per cent. deviation in the tops of the pulses from the postulated shape. In the Appendix, the ratio of the rise time to the pulse duration is shown to be inversely proportional to the number of harmonics of the pulse-width frequency included in the reproducible band. Practically, all pulses that may be encountered have finite rise and decay periods which are seldom less than 5 per cent.

of the pulse width. Therefore, the bandwidth need seldom be greater than the twentieth harmonic of the pulse-width frequency.

CURRENT-METERING RESISTOR.

For an oscillographic measurement of a current pulse, the shape of the voltage pulse developed across the metering resistor should be exactly similar to that of the current pulse. Therefore the metering resistor must have the same phase shift and amplitude characteristics

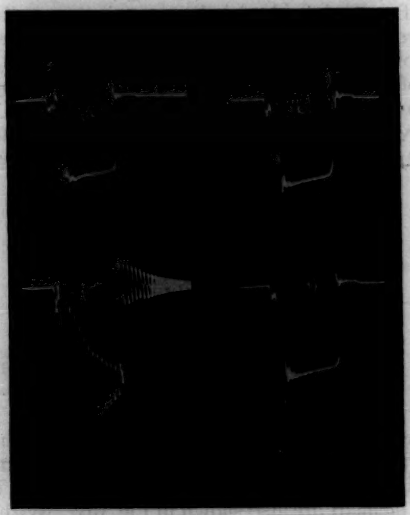

FIG. 5. Photographs of a 6 ampere, 1 microsecond current pulse repeated 1000 pulses per second.

(a) Pulse obtained with the corrected current-metering network connected with very short leads to the oscillograph.

(b) Pulse obtained with the inductive current-metering network connected with very short leads to the oscillograph.

(c) Pulse obtained with the corrected current-metering network connected with a 4-meter length of unterminated coaxial cable to the oscillograph.

(d) Pulse obtained with the corrected current-metering network connected with a 4-meter length of unterminated coaxial cable to the oscillograph.

for all frequencies contained in the band from zero to infinity. Such a resistor is physically impossible; but a network that approximates a perfect resistor over a bandwidth sufficiently great to represent the current pulse shapes to within few per cent. error can be constructed. In the measurement of large pulses of current, several watts of average

power are dissipated in the metering network. For permanency of calibration and the dissipation of power, the noninductively wound type of wire resistor should be employed as the basic element in the metering network. The frequency characteristics of a typical commercially available noninductively wound 10-watt resistor are shown in Fig. 6B. The series residual inductance exhibited by the resistor is constant over the band of frequencies of immediate importance in pulse current measurements. The wave form of the voltage across this resistor when the trapezoidal pulse of current shown in Fig. 5A is passed through it is shown in Fig. 5B. The residual inductance is responsible for the occurrence of the voltage spikes during the intervals that the pulse current has a high rate of change.

The effects of the residual inductance are corrected in the network shown in Fig. 6A. When $R_1 = R_2$, and $R_1R_2 = L_1/C$, the circuit is purely resistive with a resistance magnitude R_1 that is independent of frequency. The slight residual inductance in the resistance-capacitance

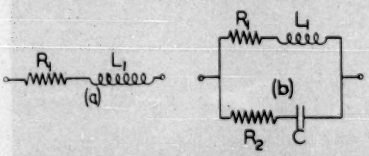

FIG. 6A. Equivalent circuits of (a) the inductive metering resistor, and (b) the same resistor connected in a frequency correcting circuit.

branch is the factor that limits the bandwidth for which the network approximates a pure resistance. The frequency characteristics for a typical network in which the inductive resistor previously discussed was used as the basic element are also shown in Fig. 6B. With this network the shape of current pulse shown in Fig. 5A was obtained. The extension of the bandwidth for the network beyond that for the inductive resistor affected elimination of the voltage spike shown in Fig. 5B, but had no effect on the remainder of the pulse. Since the bandwidth extends to 30 megacycles, this particular network may be used to view pulses of current as short as $\frac{1}{8}$ microsecond with a rise time that is 8 per cent. of the pulse width.

Practical application of this type of network is made feasible by the relative power dissipation requirements of the inductive and the capacitive branches under pulse conditions. During the pulse rise the condenser in the network charges with an efficiency of 50 per cent. through its series resistor R_2, and during the pulse decay discharges through this resistor. The energy dissipated by R_2 during the pulse rise is equal to the maximum energy that is stored in the condenser. An equal quantity

V.2
194

of energy is dissipated in R_2 during the pulse decay. Thus the total energy dissipated in R_2 per pulse is twice the maximum energy stored in the condenser. The average power loss in R_2 is the product of the repetition rate and twice the maximum energy stored in the condenser during the pulse. If the network (b) shown in Fig. 6A were used to view a 20-ampere 1-microsecond square pulse having a repetition rate of 1000 pulses per second, the power loss in R_2 would be $(CE^2) \times$ (Repetition Rate) or 0.122 watt. The remainder of the power input to the network, 5.87 watts, would be dissipated in the inductive resistor, R_1. For such a low power loss R_2 may be a 1-watt composition resistor having a sufficiently small residual inductance that the $R_2 - C$ branch of the network may effectively compensate for the inductance in R_1.

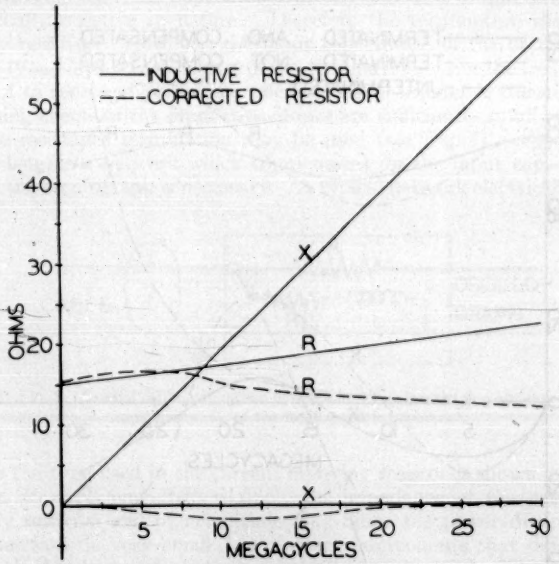

FIG. 6B. Equivalent series-circuit frequency characteristics of the inductive metering resistor and of the corrected resistor.

TRANSMISSION OF THE PULSE FROM THE RESISTOR TO THE OSCILLOGRAPH.

From the standpoint of measurement technique the leads carrying the pulse current to the metering resistor should be short, and one terminal of the metering resistor should be as near to ground potential

as possible. Therefore lengthy connections from the metering resistor to the deflection plates of the oscillograph are usually necessary. To keep the viewing circuit as free as possible from extraneous effects, the connections should be made with coaxial cable. When measurements are to be made on short pulses, considerable care must be observed in the load termination of the coaxial cable. The efficacy of the termination of a given cable may be evaluated from measurements of its input

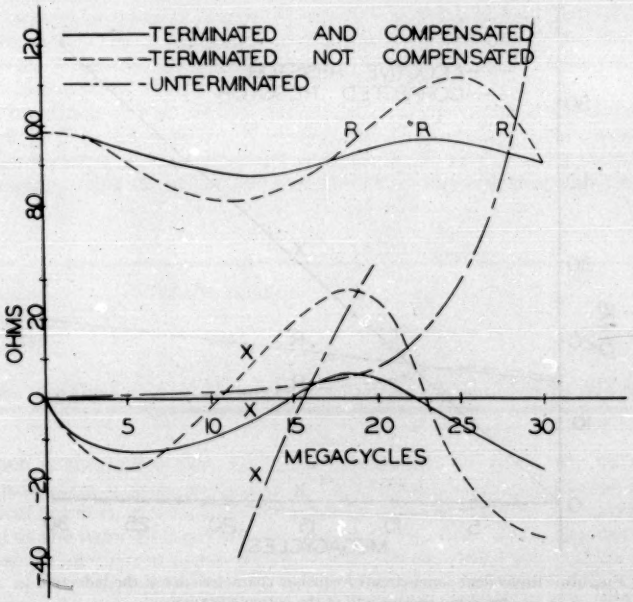

FIG. 7. Frequency characteristics of a 4-meter length of a 90-ohm coaxial cable with different terminations—(a) unterminated; (b) terminated with a single resistance; (c) terminated with the type of network shown in Figure 8.

impedance. When properly terminated, the input impedance is the characteristic impedance. When improperly terminated, the cable causes transient reflections which are superimposed upon the observed pulse and tend to obscure its shape. The amplitude of the reflections are indicated by and may be evaluated from the deviation in phase and magnitude of the input impedance from the characteristic impedance of the cable. The observed pulse when a 4-meter length of coaxial cable without termination (see Fig. 7 for the input impedance of

the cable) is used in the measurement of a trapezoidal current pulse as shown in Fig. 5C. The transient reflections make the true shape of the one microsecond pulse completely indistinguishable.

When the coaxial cable is properly terminated in its own characteristic impedance, reflections of this type are completely eliminated. In coaxial cables suited for very high frequency transmission, the attenuation at the frequencies used in pulse measurements is sufficiently low that the characteristic impedance is nearly constant in magnitude and practically resistive in nature. Therefore the termination should be purely resistive. However, the input capacitance of the oscillograph, $C_0 = 19\ \mu\mu f$ in this case, is part of the termination. For the frequencies needed to represent pulses one microsecond or greater in duration, the shunting effects of the input capacitance are sufficiently small so that a simple resistance termination may be used (see Fig. 7). For shorter pulse lengths a network which compensates for the input capacitance, C_0, of the oscillograph is necessary. A typical network electrically simi-

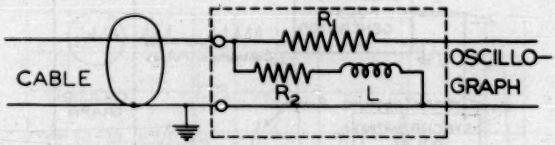

FIG. 8. Coaxial cable termination network for pulse lengths that the input capacitance, C_0, of the oscillograph is important.

lar to the type used in the current metering resistor is shown in Fig. 8. When $R_1 = R_2$ and $R_1R_2 = L/C_0$, the impedance of the network is purely resistive and of magnitude R_1. Since the power dissipated in this network is very small, low wattage components that differ little from the ideal over the pulse bandwidths may be used. The improvement in the transmission bandwidth for the pulse cable when this network is used for termination is shown by the solid line in Fig. 7. Since the bandwidth extends to 30 megacycles, the cable may be used in the measurement of pulses are short as $\frac{1}{3}$ microsecond.

SYSTEM CALIBRATION.

For measurement of the amplitude of the pulse, the deflection sensitivity of the oscillograph and the equivalent resistance of the metering network and terminated coaxial cable are required. The deflection sensitivity is measured directly at the oscillograph by observing the deflection of the beam for a known d-c. voltage. The equivalent resistance of the network and cable that is presented to the pulse is

measured at the pulse-current terminals of the network. This value measured with a Wheatstone Bridge is accurate for the bandwidth of the metering system and is equivalent to the resistance of the metering network and characteristic impedance of the terminated cable considered in parallel. When short lengths of coaxial cable are used, the attenuation of the pulse between the metering network and the oscillograph is negligible. Therefore the current sensitivity of the metering system in amperes per unit of cathode-ray deflection is the quotient of the deflection sensitivity of the oscillograph and the equivalent resistance of the metering system.

Measurement of the duration and specification of the shape of a pulse requires that the sweep of the oscillograph be calibrated against time. A circuit for calibration is shown in Fig. 9. The synchronizing pulse-generator starts the pulse generator and triggers the sweep of the oscillograph. The output of the calibration pulse generator is a series of

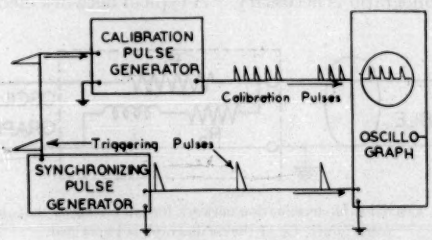

FIG. 9. Circuit for calibration of the sweep time of the oscillograph.

pulses that appear on the screen of the oscillograph and that are short in duration compared to the sweep. The time interval between the pulses shown on the screen of the oscillograph is the period of the fundamental frequency of the calibration pulse generator. If the repetition frequency of the synchronizing pulse generator is low, less than several hundred impulses per second, and if the interval of operation of the calibration pulse generator is greater than half of the interval between synchronizing impulses from the synchronizing pulse generator, the frequency of the calibration pulse generator may be measured in a conventional manner with a calibrated radio receiver. Thus the sweep of the oscillograph may be calibrated against time.

APPENDIX.

The bandwidth required for a pulse to be represented with a given accuracy may be obtained more rigorously by the use of Fourier Transforms. In this derivation the fundamental Fourier Transform rela-

tionships [1] are assumed as follows:

$$g(\omega) = \frac{1}{2\pi}\int_{\infty}^{\infty} f(t)e^{-i\omega t}dt, \tag{5}$$

$$f(t) = \int_{-\infty}^{\infty} g(\omega)e^{i\omega t}d\omega. \tag{6}$$

The time function $f(t)$ defines the disturbance that is to be analyzed. $g(\omega)$ is the corresponding frequency function that reproduces the disturbance. In this derivation $f(t)$, shown in Fig. 10A, is a repeated

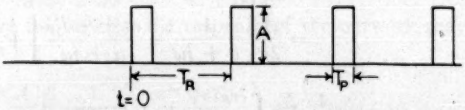

FIG. 10A. Repeated pulse wave $f(t)$ initiated at $t = 0$ and continuing thereafter.

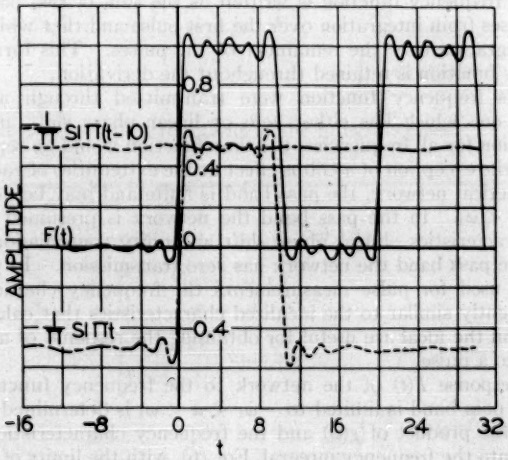

FIG. 10B. Response function $F(t)$ showing the first two pulses of $f(t)$ for the particular case that $T_R = 20$, $T_P = 10$, and the bandwith, $\omega_1 = \pi$.

pulse wave initiated at $t = 0$. In the mathematical form which is used in the transforms, the time function is defined as follows:

$$\begin{aligned} &f(t) = 0, \qquad t < 0, \qquad rT_R + T_P < t < (r+1)T_R, \\ &f(t) = Ae^{-at}, \qquad rT_R < t < rT_R + T_P, \qquad r = 0, 1, 2, 3 \cdots. \end{aligned} \tag{7}$$

The integrand in the time integral, Eq. (5), must be convergent in order for the integral to exist. The factor $e^{-\alpha t}$ was introduced into the amplitude function of the wave to satisfy the convergence requirement of the time integral. Since the constant α may be chosen small, the effect of the $e^{-\alpha t}$ term on the first few pulses in the repeated wave is negligible. The frequency function $g(\omega)$ that reproduces this wave is obtained when the function $f(t)$ defined in Eq. (7) is substituted into the infinite time integral as follows:

$$g(\omega) = \frac{1}{2\pi}\int_0^{T_P} Ae^{-(\alpha+j\omega)t}dt + \frac{1}{2\pi}\sum_{r=1}^{\infty}\int_{rT_R}^{rT_R+T_P} Ae^{-(\alpha+j\omega)t}dt$$

$$= \frac{A}{2\pi}\left[\frac{1}{\alpha+j\omega} - \frac{e^{-(\alpha+j\omega)T_P}}{\alpha+j\omega}\right] + G(\omega), \quad (8)$$

where

$$G(\omega) = \frac{1}{2\pi}\sum_{r=1}^{\infty}\int_{rT_R}^{rT_R+T_P} Ae^{-(\alpha+j\omega)t}dt.$$

Here the frequency function is written as the sum of two parts, that which arises from integration over the first pulse and that which arises from integration over the remainder of the pulses. This form of the frequency function is retained throughout the derivation.

If this frequency function were transmitted through a perfect network, one which has either zero or linear phase shift and unity transmission for all frequencies, the time function would be reproduced but with the exception of a Gibbs effect at the extremities of each pulse. For a practical network, the pass band is finite and may be defined as $-\omega_1 < \omega < \omega_1$. In the pass band the network is presumed to have ideal characteristics—linear phase shift and unity transmission. Outside of the pass band the network has zero transmission. In practical networks used for pulse measurements the frequency characteristics are sufficiently similar to the idealized characteristics that calculations based upon the ideal are useful for obtaining the response of an actual network to a pulse.

The response $F(t)$ of the network to the frequency function $g(\omega)$ when the pass band is limited to $-\omega_1 < \omega < \omega_1$ is determined by substituting the product of $g(\omega)$ and the frequency characteristics of the network into the frequency integral, Eq. (6), with the limits of integration restricted to the pass band. Thus

$$F(t) = \int_{-\omega_1}^{\omega_1} g(\omega)e^{j\omega(t-t_0)}d\omega$$

$$= \int_{-\omega_1}^{\omega_1}\frac{A}{2\pi}\left[\frac{1}{\alpha+j\omega} - \frac{e^{-(\alpha+j\omega)T_P}}{\alpha+j\omega}\right]e^{j\omega(t-t_0)}d\omega$$

$$+ \int_{-\omega_1}^{\omega_1} G(\omega)e^{j\omega(t-t_0)}d\omega. \quad (9)$$

The term, $e^{-j\omega t_0}$, where t_0 is a constant, that appears in the integral expresses the linear phase-shift and unity-response characteristics for the frequencies in the pass band of the network. By a substitution of $t - t_0$ for t in Eq. (6), the linear phase shift term $e^{-j\omega t_0}$ is shown to have the effect of delaying the network response function $F(t)$ by a time t_0. Since the magnitude of the time delay is of no importance in the remainder of the derivation, t_0 is not evaluated. In Eq. (9), the integrand for negative frequencies is conjugate to the integrand for corresponding positive frequencies. Thus by writing the integral in Eq. (9) in the form $\int_{-\omega_1}^{\omega_1} = \int_{-\omega_1}^{0} + \int_{0}^{\omega_1}$ and by substituting $-\omega$ for ω in the integral for the negative frequencies, the response of the network may be written in the form

$$F(t) = \int_0^{\omega_1} \frac{A}{2\pi}\left(\frac{1}{\alpha + j\omega} - \frac{e^{-(\alpha+j\omega)T_P}}{\alpha + j\omega}\right) e^{j\omega(t-t_0)}d\omega + \int_0^{\omega_1} \frac{A}{2\pi}\left(\frac{1}{\alpha - j\omega} - \frac{e^{-(\alpha-j\omega)T_P}}{\alpha - j\omega}\right) e^{-j\omega(t-t_0)}d\omega + \int_{-\omega_1}^{\omega_1} G(\omega)e^{j\omega(t-t_0)}d\omega. \quad (10)$$

Eliminating the complex functions in the integrals gives

$$F(t) = \frac{A}{\pi}\int_0^{\omega_1} \frac{\alpha}{\alpha^2 + \omega^2}[\operatorname{Cos}\omega(t - t_0) - e^{-\alpha T_P}\operatorname{Cos}\omega\{(t - t_0) - T_P\}]d\omega + \frac{A}{\pi}\int_0^{\omega_1} \frac{\omega \operatorname{Sin}\omega(t - t_0)}{\alpha^2 + \omega^2}d\omega - \frac{A}{\pi}\int_0^{\omega_1} \frac{\omega e^{-\alpha T_P}}{\alpha^2 + [\omega^2} \operatorname{Sin}\omega\{(t - t_0) - T_P\}d\omega + \int_{-\omega_1}^{\omega_1} G(\omega)e^{j\omega(t-t_0)}d\omega. \quad (11)$$

The damping term $e^{-\alpha t}$ was originally introduced to provide the needed convergence for the time integral. For small values of α, the first few pulses of the original time function $f(t)$ are not appreciably affected. As α is decreased, the number of pulses unappreciably effected by the $e^{-\alpha t}$ term becomes larger. As the Lim $\alpha \to 0$, $f(t)$ approaches a square pulse wave beginning at $t = 0$ and continuing for an infinite time. In the remainder of the analysis, the limiting condition of α is used.

As Lim $\alpha \to 0$, the following conditions apply to the terms in Eq. (11):

$$\lim_{\alpha\to 0}\int_0^{\omega_1}\frac{\alpha}{\alpha^2+\omega^2}\left[\cos\omega(t-t_0)-e^{-\alpha T_P}\cos\omega\{(t-t_0)-T_P\}\right]d\omega=0$$

$$\lim_{\alpha\to 0}\int_0^{\omega_1}\frac{\omega}{\alpha^2+\omega^2}\sin\omega(t-t_0)d\omega=\mathrm{Si}\,\omega_1(t-t_0) \tag{12}$$

$$\lim_{\alpha\to 0}\int_0^{\omega_1}\frac{\omega}{\alpha^2+\omega^2}\sin\omega\{(t-t_0)-T_P\}d\omega=\mathrm{Si}\,\omega_1\{(t-t_0)-T_P\}.$$

Thus the response of the network becomes

$$f(t)=\frac{A}{\pi}\left[\mathrm{Si}\,\omega_1(t-t_0)-\mathrm{Si}\,\omega_1\{(t-t_0)-T_P\}\right]+\lim_{\alpha\to 0}\int_{-\omega_1}^{+\omega_1}G(\omega)e^{j\omega(t-t_0)}d\omega. \tag{13}$$

The functions,[2] $1/\pi\,\mathrm{Si}\,\omega_1(t-t_0)$, $1/\pi\,\mathrm{Si}\,\omega_1\{(t-t_0)-T_P\}$, and the first two pulses represented by Eq. (13) are shown plotted in Fig. 10B. For values of $|\omega_1(t-t_0)|>18$, the value of $1/\pi\,\mathrm{Si}\,\omega_1(t-t_0)\simeq\pm\frac{1}{2}$. In repeated pulse waves where the time of separation between pulses is such that $\omega_1(T_R-T_P)>18$, each individual pulse may be described with negligible interference from the terms for other pulses by a term similar in form to $A/\pi[\mathrm{Si}\,\omega_1(t-t_0)-\mathrm{Si}\,\omega_1\{(t-t_0)-T_P\}]$. Under these conditions, the first term in Eq. (13) describes the first pulse in $F(t)$. The remainder of the pulses in $F(t)$ are similar in form but delayed in time from the first and are contained in the integral term of the equation. Thus the accuracy of the approximation obtained by limiting the bandwidth to $-\omega_1<\omega<\omega_1$ may be determined from the behavior of the first term in Eq. (13). For bandwidths such that the shape of the pulse is approximately trapezoidal, the slope of the tangent to the pulse at $t-t_0=0$ is about average for the rising edge of the pulse, and has the equation

$$\frac{d}{dt}F(t)\bigg|_{t-t_0=0}=\frac{A}{\pi}\frac{dt}{d}\left[\mathrm{Si}\,\omega_1(t-t_0)-\mathrm{Si}\,\omega_1\{(t-t_0)-T_P\}\right]\bigg|_{t-t_0=0}=\frac{A\omega_1}{\pi}. \tag{14}$$

The time of rise, t_{rise}, of the pulse is calculated from the slope of the tangent to the pulse at $t-t_0=0$ as follows:

$$t_{rise}=\frac{A}{\dfrac{d}{dt}F(t)\Big|_{t-t_0=0}}=\frac{\pi}{\omega_1}. \tag{15}$$

However, the accuracy of a given approximation to a pulse should be expressed in terms of the ratio K of the rise time to the duration of the pulse.

$$K=\frac{t_{rise}}{T_P}=\frac{\pi}{\omega_1 T_P}=\frac{1}{2F_1T_P}. \tag{16}$$

V. 19

In order to obtain a convenient expression for the bandwidth needed to give a desired approximation to a pulse, F_1 is replaced nF_P, where n is the harmonic of the pulse-width frequency F_P. With this substitution, Eq. (16) reduces to

$$K = \frac{1}{n}.$$

Therefore the ratio of the time of rise to the pulse width for a given repeated pulse wave is inversely proportional to the number of harmonics of the pulse-width frequency that are included in the pass band, provided that the separation between pulses is such that $\omega_1(T_R - T_P) > 18$.

REFERENCES.

1. GUILLEMIN, E. A., "Communication Networks," John Wiley & Sons, New York City, 1935, Volume II, page 461–487.
2. JAHNKE, E., AND EMDE, F., "Tables of Functions," G. Teubner, Leipzig and Berlin, 1933, page 83.

LIST OF SYMBOLS.

a_k Amplitude coefficient of the kth harmonic of F_R.
A Amplitude of the pulse in the repeated pulse wave.
C_0 Oscillograph input capacitance.
$f(t)$ The repeated pulse wave, defined differently in body and Appendix.
F_1 Frequency corresponding to ω_1.
F_P Pulse-width frequency. Has period equal to $2T_P$.
F_R Basic pulse repetition frequency. Has period equal to T_R.
$F(t)$ The response function of the network when the bandwidth is limited to ω_1.
$g(\omega)$ The frequency function corresponding to the $f(t)$ used in the transforms.
$G(\omega)$ A portion of $g(\omega)$ in the Appendix.
k Number of the harmonic of F_R.
K Ratio of the rise time to the pulse width.
m Series of positive integers which are involved in envelope of spectrum.
n Number of harmonics of pulse-width frequency included in pass band.
r The number of pulses that has occurred counted from the first.
R_1, R_2, L, C The constant in the measuring network.
t Time.
t_0 Time delay for a pulse.
T_P Duration of the pulse.
T_R Interval of time between successive pulses in the pulse wave.
ω Angular frequency.
ω_1 Limit of the pass band for the measuring networks.

Frozen Juice Like Fresh.—One of the very best of the orange juice products is a semi-concentrated juice stored at zero temperature and made ready for drinking by diluting with three parts of water to one of juice.

This is the opinion of workers at the U.S. Department of Agriculture's Winter Haven, Florida, Laboratory, who haveh ad opportunity to taste the products of many systems of processing. It was developed at the Laboratory in cooperation with the Florida Citrus Commission.

"In this method," says M. K. Veldhuis of the Bureau of Agricultural and Industrial Chemistry, "orange juice is vacuum-concentrated to about 5-fold. Then fresh juice is added to reduce the mixture to a 4-fold concentration.

"The addition of fresh juices," says Veldhuis, "replaces much of the flavor lost in the vacuum concentration process."

This 4-fold concentrate is then quick-frozen and marketed through frozen food channels. "At the usual zero storage temperature, the product is little harder than a slush and can be mixed readily with three volumes of tap water to quickly prepare a cold drink hardly distinguishable from fresh juice but with a decided gain from reducing costs for transportation and storage."

R. H. O.

X-Raying Oil Fields. (*Electrical Engineering*, Vol. 66, No. 7.)—A method of X-raying oil fields by remote operation from its research laboratories has been developed by Gulf Oil Corporation. The new development helps solve the riddle of how oil flows through the sand and rocks under any particular field, and how it is affected by underground water and gas.

Since X-raying entire oil fields at their sites would be impractical, the fields were brought to the laboratory. Small 3-inch by 1-inch samples, or cores, from the drill holes are made to reproduce in miniature the layer of rock or sand from which they were taken. Reactions studied within the samples give a picture of flow conditions in a stratum perhaps hundreds of feet thick and miles in extent.

To make such studies, the core is subjected to artificial pressures and saturations of oil, gas, and water. The progress of these elements in the core is gauged by an X-ray device for determining permeability-saturation. The X-ray beams follow the reaction by means of an opaque tracer mixed with the liquid or gas.

First step of the researcher is to establish a basis for comparison by studies of the core at 100 per cent and at zero saturation. Then an extensive series of flow experiments, reproducing conditions which might be created by various recovery methods, must be made.

Effects of gravity, capillary attraction, and the amounts of oil, gas, and water already in the sand are charted. These procedures must be repeated sometimes on as many as 10 or 11 cores taken from the different layers through which the well extends.

By correlating such data, the laboratory can determine how natural pressure, or artificial gas injection, or water flooding will move oil through various strata of the field being studied toward well shafts. Operating methods can be planned accordingly to assure the greatest yield, and the extent of the yield forecast.

Permeability-saturation determination by X-rays represents an extension of the electrolytic model oil field technique developed for predicting generalized oil field behavior and guiding placement of wells.

R. H. O.

RIGOROUS AND APPROXIMATE TREATMENT OF LONG LINE TRANSMISSION PROBLEMS BY HYPERBOLIC FUNCTIONS.*

BY

S. GERSZONOWICZ.

Professor of Electrical Engineering, University of Montevideo.

I. INTRODUCTION.

It is generally agreed that in rigorous treatment of long transmission lines hyperbolic functions must be employed. In order to facilitate the application of these functions, charts and tables have been prepared; the last chart, due to Woodruff, covers the values of $\theta^2 = ZY$ between 0.05 and 0.36, corresponding to the lengths of aerial lines between approximately 100 and 300 miles at 60 c/s, because θ/L is practically constant and equal to 0.0018–0.0022 per mile at 60 c/s.

Almost all authors state that when using the expansions in series of hyperbolic functions it is possible to obtain any precision desired by taking a sufficient number of terms. They consider however the mathematical precision only; many of them (for example, Nesbitt, Wagner and Evans, etc.) give in their books examples of computation of successive terms in order to show that these terms diminish very rapidly, so that quite soon they do not affect the first, say four, significant figures.

A reference—rather vague—to the physical problem is found in G. D. McCann's excellent chapter No. 4 in the "Westinghouse Transmission and Distribution Reference Book" (1944). McCann fixes at 0.5 per cent. the mathematical precision of the developments, because "the resistance, inductance and capacitance of a line can rarely be known within 3 or 4 per cent. and probably never within 1 per cent. This is due to conductor sag, its variation with differents spans and the variation that exists in conductor spacing, together with the effect of temperature upon conductor resistivity and sag."

In this paper we shall treat the physical aspect of the problem more comprehensively. We must consider two points:

(I) There is no physical significance in adding a new term of a development unless this term is large enough as compared to the maximum error committed in the value of the sum of preceding terms. We shall admit that it is so if a consecutive term is larger than 0.25 of the maximum error in the sum of the preceding terms. Of course, a value other than 0.25 may be chosen without affecting the generality of the treatment;

* Lecture given at the Graduate School of Engineering, Harvard University, on April 10th, 1947.

(II) Even if it makes sense to add a new term in compliance with the consideration (I), its addition may not be worthwhile in view of the limited accuracy within which a given magnitude has to be known.

As a corollary of (II) we shall examine the problem under which conditions a line may be considered short, that is of negligible capacitance. The textbooks agree that an overhead line may be considered short when it is 20 or 30 miles long; some say that the effects of capacitance may be neglected whatever the length of line, if the voltage is lower than 40 kV. We shall see that the problem cannot be stated in this simple manner.

It is easy to see, applying to the term in θ^6 the same treatment that we shall use in respect to the terms in θ^2 and θ^4, that the term in θ^6 may be omitted for present usual lengths of lines. Consequently we shall limit all developments to the terms in θ^4 and below.

II. ERRORS ON THE CONSTANTS OF A LINE.

Let, per mile,

r—the resistance, in ohms,
$l\omega$—the inductive reactance, in ohms,
$c\omega$—the capacitive susceptance, in mhos.

We shall neglect the conductance g, ordinarily very small. We have

$$\bar{Z} = Z\underline{/\gamma} = \sqrt{r^2 + l^2\omega^2}L\underline{/\arctan l\omega/r},$$

$$\bar{Y} = Y\underline{/\pi/2} = c\omega L\underline{/90^\circ},$$

where L is the length of the line in miles.

The maximum errors on Z, γ and Y are

$$\frac{\Delta Z}{Z} = \frac{\Delta r}{r}\cos^2\gamma + \frac{\Delta(l\omega)}{l\omega}\sin^2\gamma + \frac{\Delta L}{L}, \tag{1}$$

$$\Delta\gamma = \left(\frac{\Delta(l\omega)}{l\omega} + \frac{\Delta r}{r}\right)\sin\gamma\cos\gamma, \tag{2}$$

$$\frac{\Delta Y}{Y} = \frac{\Delta(c\omega)}{c\omega} + \frac{\Delta L}{L}, \tag{3}$$

and are due to the variable atmospheric conditions, the variation of frequency and of the load, and the approximation of the formulas used for the calculation of the constants, or the errors in the measurements of these constants.

III. THE EQUIVALENT π CIRCUIT.

We have

$$\bar{Z}_\pi = \bar{Z}\frac{\sinh\bar{\theta}}{\bar{\theta}} = \bar{Z}\left(1 + \frac{\bar{\theta}^2}{6} + \frac{\bar{\theta}^4}{120} + \frac{\bar{\theta}^6}{5040} + \cdots\right), \tag{4}$$

$$\bar{Y}_\pi = \frac{\bar{Y}}{2}\frac{\tanh(\bar{\theta}/2)}{(\bar{\theta}/2)} = \frac{\bar{Y}}{2}\left(1 - \frac{\bar{\theta}^2}{12} + \frac{\bar{\theta}^4}{120} - \frac{17\bar{\theta}^6}{20140} + \cdots\right). \tag{5}$$

A. The Development of $\bar{Z}_e$.

We have, limiting the development to the term in θ^4,

$$\bar{Z}_e = \bar{Z}\left(1 + \frac{\bar{\theta}^2}{6} + \frac{\bar{\theta}^4}{120}\right) \tag{6}$$

and the projections of $\bar{Z}_e$, M on $\bar{Z}$ and N on the normal to $\bar{Z}$, are (Fig. 1):

$$M = Z\left(1 - \frac{\theta^2}{6}\sin\gamma - \frac{\theta^4}{120}\cos 2\gamma\right), \tag{7}$$

$$N = Z\left(\frac{\theta^2}{6}\cos\gamma - \frac{\theta^4}{120}\sin 2\gamma\right). \tag{8}$$

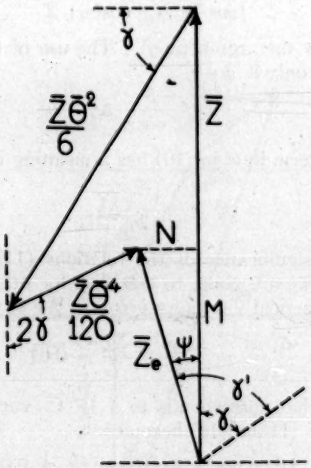

FIG. 1.

Hence

$$\tan\psi = N/M \cong \frac{\theta^2}{6}\cos\gamma + \frac{\theta^4}{180}\sin 2\gamma \cong \psi.$$

The modulus and argument of $\bar{Z}_e$ are

$$Z_e = \frac{M}{\cos\psi} \cong M(1 + \tfrac{1}{2}\tan^2\psi)$$

$$\cong Z\left[1 - \frac{\theta^2}{6}\sin\gamma - \frac{\theta^4}{120}(\cos 2\gamma - \tfrac{4}{3}\cos^2\gamma)\right], \tag{9}$$

$$\gamma' = \gamma + \psi \cong \gamma + \frac{\theta^2}{6}\cos\gamma + \frac{\theta^4}{180}\sin 2\gamma. \tag{10}$$

If the use of the second term, $(Z\theta^2 \sin\gamma)/6$, in (9) has to have any physical meaning, we must have, according to the consideration (I):

$$\tfrac{1}{4}\Delta Z \leq (Z\theta^2 \sin\gamma)/6; \quad \text{hence} \quad \theta^2 \geq \frac{3}{2\sin\gamma}\frac{\Delta Z}{Z}. \tag{11}$$

In examining the use of the third term, we should compare it with the maximum error in $Z - (Z\theta^2 \sin\gamma)/6$, but in an analysis of errors it will be sufficiently correct to compare it with the maximum error in Z only, $(Z\theta^2 \sin\gamma)/6$ being relatively small with respect to Z. Consequently, the use of the term in θ^4 in (9) has no physical meaning unless

$$\theta^4 \geq \frac{30}{|\cos 2\gamma - \frac{5}{3}\cos^2\gamma|}\frac{\Delta Z}{Z}. \tag{12}$$

Let us consider now the argument γ'. The use of the second term in (10) has a meaning only if

$$\theta^2 \geq \frac{3}{2\cos\gamma}\Delta\gamma \tag{13}$$

and the use of the term in θ^4 in (10) has a meaning if

$$\theta^4 \geq \frac{45}{\sin 2\gamma}\Delta\gamma. \tag{14}$$

To see the actual significance of the relations (11)–(14), and of the similar ones which we are going to establish for other magnitudes, we have to assume numerical values for errors. We shall admit

$$\frac{\Delta(c\omega)}{c\omega} = \frac{\Delta(l\omega)}{l\omega} = \frac{\Delta L}{L} = 0.01$$

and $\Delta r/r = 0.06$, what corresponds to a 15° C. variation in temperature. The relations (11 and 13) become:

$$\theta^2 \geq \frac{3}{2}\frac{0.06\cos^2\gamma + 0.01\sin^2\gamma + 0.01}{\sin\gamma}, \tag{11a}$$

$$\theta^2 \geq 0.105\sin\gamma. \tag{13a}$$

The relations (11a) and (13a) show that the lengths L' (modulus) and L'' (argument) for which the terms in θ^2 have to be considered in (9) and (10), respectively, depend on γ. Making $\theta = 2.10^{-3}L$, we find

modulus (11a): $L' = 85$ miles for $\gamma \cong 90°$, and 155 miles for $\gamma = 45°$;
argument (13a): $L'' = 160$ miles for $\gamma \cong 90°$, and 135 miles for $\gamma = 45°$.

Similarly, the relation (12) gives

$$L' = 450 \text{ miles for } \gamma \cong 90°, \text{ and } 600 \text{ miles for } \gamma = 45°.$$

The relation (14) gives $L'' = 550$ miles independently of γ.

Consequently for present lines the term in θ^4 should not be taken into account. It not only means that it is sufficient to make $Z_e = Z\left(1 + \frac{\bar{\theta}^2}{6}\right)$, but also that, when calculating Z_e, we do not have to correct for $1/\cos\psi$, and ought to write $Z_e = M$.

B. The Development of $\bar{Y}_e$.

We find, in similar manner as for $\bar{Z}_e$ (Fig. 2):

$$Y_e = \frac{Y}{2}\left[1 + \frac{\theta^2}{12}\sin\gamma - \frac{\theta^4}{120}\left(\cos 2\gamma - \tfrac{5}{12}\cos^2\gamma\right)\right], \qquad (15)$$

$$\tan\psi = \frac{\theta^2\cos\gamma}{12}\left(1 + \frac{7\theta^2}{60}\sin\gamma\right) \cong \frac{rLY}{12} \cong \psi. \qquad (16)$$

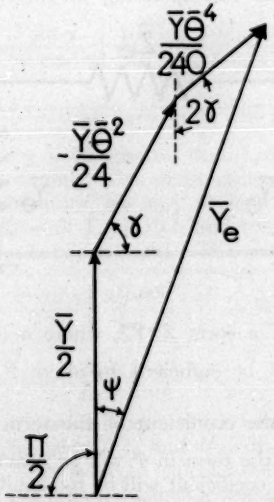

FIG. 2.

The second term in (15) will be used if

$$\theta^2 \geq \frac{3|}{\sin\gamma}\frac{\Delta Y}{Y} \qquad (17)$$

and the third one if

$$\theta^4 \geq \frac{30}{\left|\cos 2\gamma - \tfrac{5}{12}\cos^2\gamma\right|}\frac{\Delta Y}{Y}. \qquad (18)$$

Let us consider now the argument of $\bar{Y}_e$, $(90° - \psi)$. In view that we assumed $g = 0$, the term in θ^2 in (16) must always be considered, as far as only the consideration (I) is concerned.

The second term in (16) has to be considered only if

$$\theta^2 \geq \frac{15}{7 \sin \gamma}\left(\frac{\Delta r}{r} + \frac{\Delta L}{L} + \frac{\Delta Y}{Y}\right) \tag{19}$$

c.

Until now we have considered $\bar{Z}_e$ and $\bar{Y}_e$ alone, but generally it is necessary to consider them in combination with themselves and with other magnitudes. The conclusions obtained before may not be valid, because of possibility of compensation and of the presence of new terms.

We are interested in obtaining correct values of the terms in θ^2 and θ^4 in the developments corresponding to various magnitudes. Note

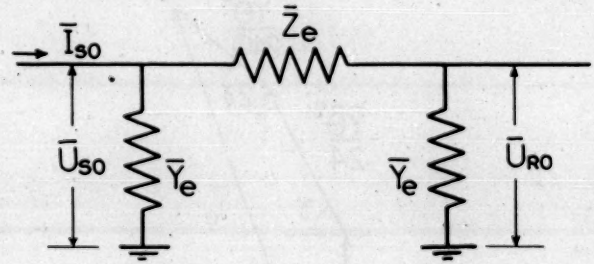

FIG. 3.

that for expression of a form $\bar{Z}_e^a \bar{Y}_e^b$, where a and b are positive integers or zero, it will be sufficient to make $\bar{Z}_e = \bar{Z}\left(1 + \frac{\delta^2}{6}\right)$ and $\bar{Y}_e = \frac{Y}{2}\left(1 - \frac{\delta^2}{12}\right)$; the coefficient of the term in δ^2 will be always exact, and the one of the term in θ^4 will be exact if $a > 0$ and $b > 0$; if $a = 0$ or $b = 0$, this coefficient will be too small in $(a + b)/120$.

If we make $\bar{Z}_e = \bar{Z}$ and $\bar{Y}_e = \bar{Y}$, the coefficient of δ^2 will be exact only if $a > 0$ and $b > 0$.

IV. LINE AT NO LOAD. RELATION OF THE VOLTAGES.

We have (Fig. 3):

$$\frac{\bar{U}_{SO}}{\bar{U}_{RO}} = 1 + \bar{Z}_e \bar{Y}_e = \bar{A} = A/\underline{\delta}, \tag{20}$$

where $\bar{A}$ is one of the constants $\bar{A}$, $\bar{B}$, $\bar{C}$ and $\bar{D} = \bar{A}$ of the equivalent four terminal network.

Let us make in (20) $\bar{Z}_e = \bar{Z}\left(1 + \frac{\bar{\theta}^2}{6}\right)$ and $\bar{Y}_e = \frac{\bar{Y}}{2}\left(1 - \frac{\bar{\theta}^2}{12}\right)$, we obtain

$$\bar{A} = 1 + \frac{\bar{\theta}^2}{2} + \frac{\bar{\theta}^4}{24}, \tag{21}$$

where the coefficient of $\bar{\theta}^4$ is exact, according to what we said above.

The modulus is

$$A = \frac{U_{SO}}{U_{RO}} = 1 - \frac{\theta^2}{2}\sin\gamma - \frac{\theta^4}{24}(\cos 2\gamma - 3\cos^2\gamma) \tag{22}$$

and there is a meaning in using the term in θ^4 if this term is larger than 0.25 of the error in the term in θ^2, that is, if

$$\theta^2 \geq \frac{3\sin\gamma}{1 + \cos^2\gamma}\left[\frac{\Delta(l\omega)}{l\omega} + \frac{\Delta L}{L} + \frac{\Delta Y}{Y}\right]. \tag{23}$$

If $\frac{\Delta(l\omega)}{l\omega} + \frac{\Delta L}{L} + \frac{\Delta Y}{Y} = 0.04$, for $\gamma \cong 90°$ the length must be greater than 175 miles, and for $\gamma = 45°$ greater than 120 miles.

The value of A is obtained with great accuracy by means of (22); for example, if $L = 120$ miles, we may neglect the term in θ^4 (which means here to make $\bar{Z}_e = \bar{Z}$, $\bar{Y}_e = \bar{Y}/2$, and $\cos\delta = 1$) and the maximum error on A will be between ϵ and $1.25\,\epsilon$, with

$$\epsilon = \frac{\theta^2\sin\gamma}{2}\left[\frac{\Delta(l\omega)}{l\omega} + \frac{\Delta L}{L} + \frac{\Delta Y}{Y}\right]. \tag{24}$$

For $L = 120$ miles, and $\frac{\Delta(l\omega)}{l\omega} + \frac{\Delta L}{L} + \frac{\Delta Y}{Y} = 0.04$, $\epsilon \cong 0.001$. But normally it is sufficient that A have a much less accuracy. Indeed, if we determine A by measuring U_{SO} and U_{RO} on the respective switchboard voltmeters, it is impossible to expect to obtain A within a maximum error less than 2 per cent. In such a case it is useless to take into account the term $(\theta^2\sin\gamma)/2$ if it is smaller than 0.02, that is, if $\sin\gamma \cong 1$, for lines of less than 100 miles. Then, under the conditions just exposed a line up to 100 miles has to be considered as "short."

V. LINE AT NO LOAD. CURRENT AND POWER AT THE SENDING END.

A. Current at the Sending End.

We have (Fig. 3)

$$\frac{\bar{I}_{SO}}{\bar{U}_{SO}} = \bar{Y}_e\frac{2 + \bar{Z}_e\bar{Y}_e}{1 + \bar{Z}_e\bar{Y}_e} = \frac{\bar{C}}{\bar{A}}. \tag{25}$$

Let us make $\bar{Z}_e = \bar{Z}\left(1 + \frac{\bar{\theta}^2}{6}\right)$ and $\bar{Y}_e = \frac{\bar{Y}}{2}\left(1 - \frac{\bar{\theta}^2}{12}\right)$; we find

$$\frac{\bar{I}_{so}}{\bar{U}_{so}} = \bar{Y}\left(1 - \frac{\bar{\theta}^2}{3} + \frac{\bar{\theta}^4}{8}\right) \tag{26}$$

with an error in the coefficient of $\bar{\theta}^4$ equal to 1/120; the exact value of this coefficient is 2/15.

The modulus of I_{so}/U_{so} is

$$\frac{I_{so}}{U_{so}} = Y\left[1 + \frac{\theta^2}{3}\sin\gamma - \tfrac{2}{15}\theta^4(\cos 2\gamma - \tfrac{5}{12}\cos^2\gamma)\right] \tag{27}$$

and there only is a meaning in using the term in θ^4 if

$$\theta^4 \geq \frac{15}{8}\frac{1}{|\cos 2\gamma - \frac{5}{12}\cos^2\gamma|}\frac{\Delta Y}{Y}, \tag{28}$$

that is, if $\Delta Y/Y = 0.02$, 220 miles for $\gamma \cong 90°$ and 320 miles for $\gamma = 45°$. For any length shorter than defined by equation (28) we may write

$$\frac{I_{so}}{U_{so}} = Y\left(1 + \frac{\theta^2}{3}\sin\gamma\right) \tag{29}$$

with a maximum error between $\Delta Y/Y$ and $1.25\,\Delta Y/Y$.

To neglect the term in θ^4 is not equivalent here to make $\bar{Z}_e = \bar{Z}$ and $\bar{Y}_e = \bar{Y}/2$. If we limit the developments of $\bar{Z}_e$ and $\bar{Y}_e$ to their first terms, we find

$$\frac{I_{so}}{U_{so}} = Y\left(1 + \frac{\theta^2}{4}\sin\gamma\right) \tag{30}$$

with a supplementary negative error $(\theta^2 \sin\gamma)/12$.

If it is sufficient to obtain I_{so}/U_{so} with an even less accuracy, we may write, neglecting $\bar{Z}_e\bar{Y}_e$ compared to 1,

$$\frac{I_{so}}{U_{so}} = 2Y_e = Y\left(1 + \frac{\theta^2}{12}\sin\gamma\right) \tag{31}$$

with a supplementary negative error $(\theta^2 \sin\gamma)/4$, or

$$\frac{I_{so}}{U_{so}} = Y \tag{32}$$

with a supplementary negative error of $(\theta^2 \sin\gamma)/3$. We have now to investigate when a line may be considered as "short" from the point of view of the no-load current. In order to give a physical significance to this problem we must refer I_{so} to the load current I_n. Assume that the line is transmitting its "natural" power, magnitude introduced by Rüdenberg to characterize a load for which the line operates at nearly

its maximum efficiency. Under these conditions

$$P = 3U_R^2 \Big/ \sqrt{\frac{Z \sin \gamma}{Y}} \tag{33}$$

and hence

$$I_n = U_R \cos \varphi_R \Big/ \sqrt{\frac{Z \sin \gamma}{Y}}, \tag{34}$$

where $\cos \varphi_R$ is the power factor of the receiver.

From (32) and (34)

$$\frac{I_{SO}}{I_n} = \frac{U_{SO}}{U_R} \frac{\sqrt{\sin \gamma}}{\cos \varphi_R} \theta \cong \frac{U_{SO}}{U_R} \frac{\sqrt{\sin \gamma}}{\cos \varphi_R} 2.10^{-3} L \tag{35}$$

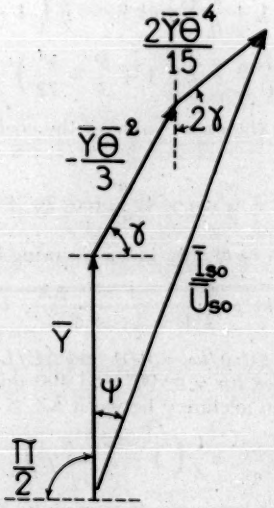

FIG. 4.

with L in miles. $U_{SO}\sqrt{\sin \gamma}/U_R \cos \varphi_R$ is nearly equal to 1; consequently we find that to call a line of a length less than 20 miles "short" means to neglect a no-load current equal approximately to 5 per cent of the full-load current.

B. Power at the sending end.

We have, calling ψ the angle between $\bar{I}_{SO}/\bar{U}_{SO}$ and $\bar{Y}$ (Fig. 4):

$$\frac{P_{SO}}{U_{SO}^2} = \frac{I_{SO}}{U_{SO}} \sin \psi = Y \left(\frac{\theta^2}{3} \cos \gamma + \frac{2\theta^4}{15} \sin 2\gamma \right) \tag{36}$$

and the use of the term in θ^4 has a meaning if

$$\theta^2 \geq \frac{5}{16 \sin \gamma}\left(\frac{\Delta r}{r} + \frac{\Delta L}{L} + \frac{2\Delta Y}{Y}\right), \tag{37}$$

that is, if $\Delta r/r + \Delta L/L + 2\Delta Y/Y = 0.11$ and $\sin \gamma \cong 1$, for lengths greater than 90 miles.

VI. LINE IN SHORT-CIRCUIT. CURRENT AT THE SENDING END.

We have

$$\frac{\bar{I}_{ss}}{\bar{U}_{ss}} = \frac{1 + \bar{Z}_e \bar{Y}_e}{\bar{Z}_e} = \frac{\bar{A}}{\bar{B}}. \tag{38}$$

Let us make $\bar{Z}_e = \bar{Z}\left(1 + \frac{\bar{\theta}^2}{6}\right)$ and $\bar{Y}_e = \frac{\bar{Y}}{2}\left(1 - \frac{\bar{\theta}^2}{12}\right)$; we obtain

$$\frac{\bar{I}_{ss}}{\bar{U}_{ss}} = \frac{1}{\bar{Z}}\left(1 + \frac{\bar{\theta}^2}{3} - \frac{\bar{\theta}^4}{72}\right) \tag{39}$$

with an error of $\bar{\theta}^4/120$; the exact value of the coefficient of $\bar{\theta}^4$ is $-1/45$. The modulus is

$$\frac{I_{ss}}{U_{ss}} = \frac{1}{Z}\left[1 - \frac{\theta^2}{3}\sin\gamma + \frac{\theta^4}{45}\left(\cos 2\gamma + \tfrac{5}{2}\cos^2\gamma\right)\right] \tag{40}$$

and the use of the term in θ^4 only has a meaning if

$$\theta^4 \geq \frac{45}{4}\frac{1}{1 + \frac{1}{2}\cos^2\gamma}\frac{\Delta Z}{Z}, \tag{41}$$

that is, if $\Delta r/r = 0.06$, $\Delta(l\omega)/l\omega = 0.01$ and $\Delta L/L = 0.01$, if the length is greater than 350 miles for $\gamma \cong 90°$ and 400 miles for $\gamma \cong 45°$. We may then write, with an accuracy between $\Delta Z/Z$ and $1.25\ \Delta Z/Z$,

$$\frac{I_{ss}}{U_{ss}} = \frac{1}{Z}\left(1 - \frac{\theta^2}{3}\sin\gamma\right). \tag{42}$$

If we may tolerate a larger error, we can make $\bar{Z}_e = \bar{Z}$ and $\bar{Y}_e = \bar{Y}/2$, obtaining

$$\frac{I_{ss}}{U_{ss}} = \frac{1}{Z}\left(1 - \frac{\theta^2}{2}\sin\gamma\right), \tag{43}$$

the supplementary error being negative and equal to $(\theta^2 \sin\gamma)/6$.

We may also simplify (38) neglecting $\bar{Z}_e\bar{Y}_e$ compared to 1; we find

$$\frac{I_{ss}}{U_{ss}} = \frac{1}{Z_e} = \frac{1}{Z}\left(1 + \frac{\theta^2}{6}\sin\gamma\right) \tag{44}$$

with a supplementary positive error $(\theta^2 \sin\gamma)/2$.

Finally, let us observe that the simplest expression for I_{SS}/U_{SS},

$$\frac{I_{SS}}{U_{SS}} = \frac{1}{Z}, \tag{45}$$

is equivalent to the consideration of the line as "short." It leads to a supplementary positive error of $(\theta^2 \sin \gamma)/3$. If we want to find I_{SS}/U_{SS} within a total accuracy of 10 per cent., with $\Delta r/r = 0.06$, $\Delta(l\omega)/l\omega = 0.01$, $\Delta L/L = 0.01$ and $\sin \gamma \cong 1$, the length should be less than about 240 miles. For 300 miles, using (45), the total error would be = 14 per cent. if $\gamma \cong 90°$, 13 per cent. of $\gamma = 45°$.

VII. LINE AT LOAD.

A. Relation of the Voltages.

We have

$$\frac{\bar{U}_S}{\bar{U}_R} = 1 + \bar{Z}_e\bar{Y}_e + \bar{Z}_e\bar{Y}_c = \bar{A} + \bar{B}\bar{Y}_c, \tag{46}$$

where $\bar{Y}_c$ is the admittance of the load.

Let us make $\bar{Z}_e = \bar{Z}\left(1 + \frac{\bar{\theta}^2}{6}\right)$ and $\bar{Y}_e = \frac{\bar{Y}}{2}\left(1 - \frac{\bar{\theta}^2}{12}\right)$; we find

$$\frac{\bar{U}_S}{\bar{U}_R} = 1 + \bar{\theta}^2\left(\frac{1}{2} + \frac{\bar{Y}_c}{\bar{Y}}\right) + \frac{\bar{\theta}^4}{6}\left(\frac{1}{4} + \frac{\bar{Y}_c}{\bar{Y}}\right). \tag{47}$$

If the power transmitted is the natural power of the line, we have

$$Y_c = \sqrt{\frac{Y}{Z \sin \gamma}} \cos \varphi_R, \qquad \text{and} \qquad \frac{Y_c}{Y} = \frac{\cos \varphi_R}{\sqrt{\sin \gamma}} \frac{1}{\theta}. \tag{48}$$

For $\cos \varphi_R \cong 1 \cong \sin \gamma$, and a length of 300 miles, $Y_c/Y = 1.6$, so that we may admit, only for the purpose of discussion of errors,

$$\frac{1}{2} + \frac{\bar{Y}_c}{\bar{Y}} \cong \frac{1}{4} + \frac{\bar{Y}_c}{\bar{Y}} \cong \frac{\bar{Y}_c}{\bar{Y}} = \frac{Y_c}{Y}\underline{/-\varphi_R - \pi/2}.$$

For the same purpose we may neglect the correction of the cosine of the angle between 1 and $\bar{U}_S/\bar{U}_R$, and find the following approximate expression for the modulus of $\bar{U}_S/\bar{U}_R$:

$$\frac{U_S}{U_R} = 1 + ZY_c \cos(\gamma - \varphi_R) - \frac{\theta^2 Z Y_c}{6} \sin(2\gamma - \varphi_R), \tag{49}$$

and the use of the third term in (49) only has a meaning if

$$\theta^2 \geq \frac{3}{2 \sin(2\gamma - \varphi_R)}\left[\frac{\Delta L}{L}\cos(\gamma - \varphi_R) + \frac{\Delta r}{r}\cos\gamma \cos\varphi_R + \frac{\Delta(l\omega)}{l\omega}\sin\gamma \sin\varphi_R\right], \tag{50}$$

for example, if $\gamma \cong 70°$, $\varphi_R \cong 25°$, $\Delta r/r = 0.06$, $\Delta(l\omega)/l\omega = 0.01 = \Delta L/L$, for $L \geq 110$ miles. For lengths less than the one defined by (50), we may make $\bar{Z}_e = \bar{Z}$ and $\bar{Y}_e = \bar{Y}/2$ in (46), which is equivalent to neglecting the third term in (47). For greater lengths all depends on the accuracy within which we want to know the relation U_S/U_R. For a line of 300 miles, to neglect the term in θ^4 in (49) is equivalent to a positive error equal to 0.02 Y_c/Y, that is, about 3 per cent. if the natural power is transmitted. It must be observed that this error is proportional to the fourth power of the length, L^4.

B. Relation of the Currents.

We have

$$\frac{\bar{I}_S}{\bar{I}_R} = 1 + \bar{Z}_e\bar{Y}_e + \bar{Z}_c\bar{Y}_e(2 + \bar{Z}_e\bar{Y}_e) = \bar{A} + \bar{C}\bar{Z}_c, \tag{51}$$

where $\bar{Z}_e$ is the impedance of the load. Let us make $\bar{Z}_e = \bar{Z}\left(1 + \frac{\bar{\theta}^2}{6}\right)$ and $\bar{Y}_e = \frac{\bar{Y}}{2}\left(1 - \frac{\bar{\theta}^2}{12}\right)$; we find

$$\frac{\bar{I}_S}{\bar{I}_R} = 1 + \bar{\theta}^2\left(\frac{1}{2} + \frac{\bar{Z}_c}{\bar{Z}}\right) + \frac{\bar{\theta}^4}{6}\left(\frac{1}{4} + \frac{\bar{Z}_c}{\bar{Z}}\right). \tag{52}$$

If the line transmits the natural power

$$\frac{Z_c}{Z} = \frac{\sqrt{\sin\gamma}}{\cos\varphi_R}\frac{1}{\theta}, \tag{53}$$

that is, for a line of 300 miles, $\sin\gamma \cong 1$ and $\cos\varphi_R \cong 1$, $\bar{Z}_c/\bar{Z} = 1, 6/\underline{\varphi_R - \gamma}$, so that we may still make for the purpose of the discussion of errors

$$\frac{1}{2} + \frac{\bar{Z}_c}{\bar{Z}} \cong \frac{1}{4} + \frac{\bar{Z}_c}{\bar{Z}} \cong \frac{\bar{Z}_c}{\bar{Z}}.$$

Furthermore we may neglect for the same purpose the correction of the cosine of the angle between 1 and $\bar{I}_S/\bar{I}_R$, and find the following approximate expression for the modulus of $\bar{I}_S/\bar{I}_R$:

$$\frac{I_S}{I_R} = 1 - Z_cY\sin\varphi_R - \frac{Z_cY\theta^2}{6}\cos(\gamma + \varphi_R). \tag{54}$$

Here the third term has a meaning if

$$\theta^2 \geq \frac{3}{2}\frac{\Delta Y}{Y}\frac{\sin\varphi_R}{|\cos(\gamma + \varphi_R)|}, \tag{55}$$

that is, if $\Delta Y/Y = 0.02$, $\gamma \cong 70°$ and $\varphi_R \cong 25°$, for lengths greater than 200 miles. Furthermore it may often be neglected because we only need to know I_S/I_R within a limited accuracy. For a line of 300 miles,

and for $\cos(\gamma + \varphi_R)$ as high as 0.5 the error in neglecting the third term, thus making $\bar{Z}_e = \bar{Z}$ and $\bar{Y}_e = \bar{Y}/2$ in (51), is positive and lower than 2 per cent.

VIII. LINE AT LOAD. POWER CIRCLES AT SENDING AND RECEIVING ENDS.

We have

$$\frac{\bar{P}_S}{U_S^2} = \frac{1 + \bar{Z}_e\bar{Y}_e}{\bar{Z}_e} - \frac{\bar{U}_R}{\bar{U}_S}\frac{1}{\bar{Z}_e} = \frac{\bar{A}}{\bar{B}} - \frac{1}{\bar{B}}\frac{\bar{U}_R}{\bar{U}_S} \tag{56}$$

and

$$\frac{\bar{P}_R}{U_R^2} = \frac{\bar{U}_S}{\bar{U}_R}\frac{1}{\bar{Z}_e} - \frac{1 + \bar{Z}_e\bar{Y}_e}{\bar{Z}_e} = \frac{\bar{U}_S}{\bar{U}_R}\frac{1}{\bar{B}} - \frac{\bar{A}}{\bar{B}}. \tag{57}$$

The modulus of the relation $\bar{A}/\bar{B}$ has been studied in VI. We found that in practically all cases it is sufficient to take

$$\frac{A}{B} = \frac{1}{Z}\left(1 - \frac{\theta^2}{3}\sin\gamma\right) = \frac{1}{Z}\left(1 - \frac{l\omega LY}{3}\right). \tag{58}$$

The argument of $\bar{A}/\bar{B}$ is

$$\gamma'' = -\gamma + \frac{\theta^2}{3}\cos\gamma(1 + \tfrac{7}{15}\theta^2\sin\gamma), \tag{59}$$

where the use of the term in θ^4 only has a meaning if

$$\theta^4 \geq \frac{45}{28}\left[\frac{\Delta(l\omega)}{l\omega} + \frac{\Delta r}{r}\right], \tag{60}$$

that is, for $\Delta(l\omega)/l\omega + \Delta r/r = 0.07$, for $L > 280$ miles.

We may then write for all usual cases

$$\gamma'' = -\gamma + \frac{\theta^2}{3}\cos\gamma = -\gamma + \frac{rLY}{3}. \tag{61}$$

For the radii, $\frac{U_S}{U_R}\frac{1}{Z_e}$ and $\frac{U_R}{U_S}\frac{1}{Z_e}$, according to the study done in III, is practically always sufficient to write

$$Z_e = Z\left(1 - \frac{l\omega LY}{6}\right). \tag{62}$$

The zero position of the radii, for which $\bar{U}_S$ and $\bar{U}_R$ are in phase, is defined by

$$-\gamma' = -\gamma - \frac{\theta^2}{6}\cos\gamma = -\gamma - \frac{rLY}{6} \tag{63}$$

The relations (58), (61), (62) and (63) determine the centers and radii of the circles of power with all the accuracy which has physical meaning for lines up to 300 miles, and without any necessity of using the hyperbolic functions.

CONCLUSIONS

We have shown that because of the errors in the constants of the line, generally there is no physical meaning in using more than two terms in the developments of $\bar{Z}_e$ and $\bar{Y}_e$. Furthermore, because it is of no use to try to determine the magnitudes beyond a certain accuracy, in many cases it is perfectly correct to limit the expansions of $\bar{Z}_e$ and $\bar{Y}_e$ to the first terms, that is $\bar{Z}$ and $\bar{Y}/2$, respectively.

The definition of a line as a "short" (of negligible capacitance) if the length is less than a given value, is not rational. It is necessary to specify the criterion employed. We have seen that a line is "short" if

$L \leq$ 20 miles	by the condition of neglecting $I_{SO} \approx 0.05\, I_n$,	(V)
$L \leq$ 100 miles	by the condition $U_{SO}/U_{RO} \geq 0.98$,	(IV)
$L \leq$ 240 miles	by the condition I_{SS}/U_{SS} exact within 10 per cent.,	(VI)

for specified values of γ, $\Delta r/r$, $\Delta(l\omega)/l\omega$, $\Delta L/L$.

NOTES FROM THE NATIONAL BUREAU OF STANDARDS.*

DETECTION OF ISOTOPES BY TRACER MICROGRAPHY.

A new method for the more effective tracing of radioactive isotopes in materials in which they have been intentionally introduced has been developed by L. Marton of the National Bureau of Standards with the cooperation of P. H. Abelson of the Department of Terrestrial Magnetism, Carnegie Institution of Washington. In this procedure, by means of a magnetic focusing arrangement, the radiation given off by a radio-isotope within a sample material is made to form an image of the emitting surface upon a photographic plate. This image may then be used in studying the distribution and concentration of the radioactive element present in the sample.

In many chemical, biological, biochemical, and other fields of research, there is growing application of the method of tracers, in which the isotope of a given element is used as an indicator to tag or label certain groups of atoms so that they may be distinguished from other atoms of the same kind. Identification of tracer elements is at present greatly facilitated through the use of radioactive isotopes, which, because of recent developments in atomic energy, are now available in large quantities and are relatively easy to detect through their radiations.

In the well-known method of radio autography a radio-isotope is introduced in a biological or other system, and the distribution of that particular element within the system is determined by bringing the sample in close contact with a photographic emulsion. This method lacks resolving power because, even in case of perfect contact of the sample with the emulsion, the circle of confusion from every point of emission is so great that details less than a tenth of a millimeter are very difficult or impossible to distinguish.

In order to improve the resolution of this tracer method, it was decided to use electron optical image formation for determination of the distribution of a radioactive element within a given sample. This process, which may be called "tracer micrography," is based on the emission of high speed electrons (beta rays) by many tracer elements and the use of magnetic lens elements to form an image on a suitable recording surface.

In the absence of any means for correction of the chromatic aberration of electron optical lenses, the first micrographs were limited to those elements which emit electrons of uniform speed. After some at-

* Communicated by the Director.

tempts with Columbium^{93}, Yttrium^{87}, Strontium^{85}, Strontium^{87}, and Protactinium^{233}, Gallium^{67} was selected for the initial tests. Gallium chloride, prepared by chemical separation from zinc, was bombarded by heavy hydrogen nuclei in the cyclotron at the Carnegie Institution, and the solution was evaporated drop after drop on a ¼-inch tantalum disc. Radiation emitted from the surface of the disc, upon passing through a magnetic lens consisting of a small ironclad coil with Armco iron pole pieces, was brought to a focus upon a photographic film at a distance of about 3½ inches. An image of the tantalum disc was thus obtained showing radioactive areas. The conditions were selected so that a linear magnification of 2 was obtained.

For calibration of the instrument, the photographic film was replaced by a Geiger counter, and the lens current necessary to produce a maximum number of counts in unit time was determined for radiations of varying velocities. This establishes the focusing current for a given type of radiation.

In preliminary experiments with samples of different concentration and thickness of the radioactive layer, exposure times ranged from 2 to 12 hours according to the age and concentration of the sample and the numerical aperture of the lens. It was found that micrographs with good definition were obtained consistently when the layer was sufficiently thin to avoid considerable self-absorption. The best resolving power attained so far has been about 30 microns.

The simplicity of this method, both in apparatus and technic, is one of its more important features. Vacuum requirements are very moderate, since the mean free path of the electrons is large in comparison with the apparatus dimensions, even at forepump pressure.

Further improvements in tracer micrography are expected through after-acceleration of the beta particles by means of an homogeneous electrostatic field. Such after-acceleration may well result in reduced exposure time and in better resolution due to a reduction in spherical aberration. A further reason for after-acceleration is that chromatic aberration, which is always present, even in sources emitting particles of uniform speed, can be markedly decreased if the accelerating potential is at least comparable in magnitude to the energy of the primary emission.

Location of radioactive tracer elements is facilitated by a new electron optical method, "tracer micrography."

TEMPERATURE DISTRIBUTION IN A TEST BUNGALOW.

Uniformity of temperature throughout houses is a tacitly accepted American ideal of heating. It is probably never attained in practice, and departures from it depend upon the design and construction of the house and upon the characteristics of the heating system or device used.

Distribution of warmth in houses has usually been judged only qualitatively by individual engineers on the basis of personal experience or observation. Quantitative data have been limited almost entirely to laboratory tests on parts of the system. In order to obtain data on the temperature distribution in an entire house, a series of heat distribution tests of several types of heating systems were conducted at the National Bureau of Standards by Richard S. Dill and Paul R. Achenbach.

A full scale house in which complete heating systems can be installed was constructed at the Bureau. Designated as a test bungalow, it is similar in plan to house B described in F.H.A.'s Technical Bulletin No. 4, "Principles of Planning Small House." It has four rooms and bath, with a central hallway. The walls are conventional in construction consisting of ½-inch gypsum board on the inside and 2- by 4-inch studding with sheathing and lap siding on the outside, separated by a layer of building paper. All the windows are double hung with the exception of that in the bathroom, and one of the two in the kitchen. The double floor of 1-inch pine includes building paper between the subfloor and finish floor. For the heat distribution tests the walls were not insulated but a 2-inch blanket of wood-fiber insulating material was laid over the ceiling. Weather-stripping is not provided for windows or doors.

During the tests, data on temperature conditions inside the bungalow were recorded by various types of instruments. Heat-transfer coefficients for floors, side walls and ceilings were measured by the Nicholls type of heat-flow meters fastened to the surfaces. Thermocouples located at various levels of the rooms, on top and bottom of the floor, on the inside and outside of the walls, and in the basement and attic air, gave a complete record of temperature conditions. Observations were made while heat was being supplied in turn by an experimental electric heater, an oil-burning warm-air furnace, a jacketed gas-firing space heater, a jacketed oil-fired space heater, a single gas-burning gravity floor furnace, two gas-burning gravity floor furnaces, a gas-burning floor furnace with forced circulation, an oil-burning gravity floor furnace, and a conventional gravity hot-water heating system.

From the standpoint of comfort, the temperatures from the floor to 5 feet above the floor are more significant than the temperatures at higher levels. The tests showed that the average temperature differences produced in the test bungalow between the 2-inch level and the 60-inch level, with continuous forced circulation of air through a plenum chamber, with a forced-circulation gas floor furnace, and with a gravity hot-water heating system, were less than 10° F. when the outside temperature was 32° F. The temperature differences produced in this same zone by all the other devices tested ranged from 14 to 18° F. at comparable outside temperatures.

The average horizontal temperature differences between rooms at

all levels of measurement ranged from 2° to 4° F. for the several floor furnaces and for the gravity hot-water system. For the electric warm-air furnace and the oil-burning furnace, when attached to a plenum chamber, these differences were nearly as small for the 2-, 30-, and 60-inch levels, but were considerably greater in the upper levels of the house. The temperature difference between rooms was greater for the space heaters in the living room than for the other heaters tested. This effect can probably be attributed to the fact that the rooms other than the one containing the heater are warmed by the overflow of heat from the living room through the doorways. Except for the space heaters, the average horizontal temperature differences from 2 inches to 60 inches above the floor did not increase with lower outside temperatures.

Certain types of heaters may be suitable for houses of one construction and not suitable for other constructions. For example, a high temperature near the ceiling would not cause much additional heat loss if the ceiling were well insulated, or an insulated floor might permit the use of heaters that do not deliver warmed air at or near the floor level. Furthermore, some types of heaters that provide comfort in areas where extremely low temperatures do not occur may not provide comfort in colder climates.

Although standards of performance in the field of vertical or horizontal temperature differences in residences have not been established, the Bureau tests indicated that the air temperatures in the living zone of all rooms should be in the range from 65° to 80° F, for comfort when heated by the conventional types of heating systems. A floor temperature of 60° F., when continued for 1 hour or more, was found to be too low for foot comfort; when a floor temperature of 65° F, was continued for the same period, discomfort was no longer apparent. It was further observed that air temperatures of approximately 85° F. around the level of the head became oppressive, especially if the air had an appreciable velocity.

The results obtained with the devices used in the test bungalow show need for further improvement in the design of house construction and heating systems in order to provide comfort in all rooms of basementless houses. A more uniform temperature can probably be obtained either by the use of more insulation in the house elements, by improving the heat-distribution systems, or by a combination of both.

Entire heating systems were installed in this test bungalow, constructed by the Bureau for studies of heat transfer phenomena, in order to determine the performance of various heating devices designed for use in low-cost housing. The bungalow is now enclosed with an insulated shell so that any desired temperature can be maintained outside of the house.

NOTE: The complete technical report on this project is contained in the National Bureau of Standards Building Materials and Structures Report BMS108, "Temperature Distribution in a Test Bungalow with Various Heating Devices."

MERCURY-BALANCE METHOD FOR THE MEASUREMENT OF GEL STRENGTH.

An improved method for more precise measurements of the tensile strength of gels [1] has been developed by W. J. Hamer of the Bureau's electrochemistry laboratory. This procedure, which gives the strength or "yield value" and resistance to deformation of the material under study, essentially involves the determination of the shearing force necessary to fracture the gel as given by the weight of mercury required to pull a standard disc from the gel in which it is embedded.

In many applications of gelatin, glue, starch, agar, and various gums, it is important to know the tensile strength of the gel or jelly. This property was originally measured by comparison with a set of arbitrary standards on the basis of the resistance offered by the gel to finger pressure. Although this procedure was undoubtedly satisfactory for many commercial purposes, there was need for a more objective method. Such a method is very important, for example, in studies of gelatin coatings in photographic operations, particularly with the increasing use of flexible film supports instead of rigid glass bases.

The new Bureau development represents objective method for gel-strength measurement. While this procedure was designed specifically for the study of the paste walls of dry cells, it may be applied to all types of gels and used in the study of food starches, in following small changes in starch pastes for use in adhesives, and in many other applications.

The method involves the balancing of the cohesive forces of the gel against a gradually increasing quantity of mercury until the yield point is reached and the gel is broken. A brass disc is suspended in a beaker containing the gel by means of a wire attached to one beam of an analytical balance. An adjustable platform over the balance pan supports the beaker. The gel is covered with liquid petrolatum to prevent "skin" formation. Mercury is added from a burette at a constant rate to a container on the other pan. Different flow rates are made possible by use of a removable capillary tip held to the burette by a rubber tube. The capillary tip is calibrated before use by weighing the mercury it delivers in a given time. As the mercury is added, the height of the platform is changed manually, so that the pointer of the balance is always kept at zero. A vertical scale indicating the height of the adjustable platform is read at frequent regular intervals until the gel is broken.

The weight of mercury required to produce a fracture in the gel divided by the area of the brass disc gives gel strength in grams per square centimeter. The rate of change in height of the adjustable platform gives an indication of the resistance the gel offers to deformation. A fast rate means that the gel is easily deformed, whereas a

[1] Details of this work are described in Bureau Research Paper RP1810, an improved method for measurement of gel strength and data on starch gels. W. J. Hamer, *J. Research*, NBS 39 (1947).

slow rate indicates that the gel resists deformation and is probably quite rigid. Although rigid gels usually offer high resistance to deformation, this is not always true.

This method has a precision greater than 0.5 per cent. Its limitations lie more in the reproducibility with which gels can be prepared than in errors inherent in the method. It may be applied to all types of gels, whether they are of the reversible (gelatin) or irreversible (starch) type.

Gel-strength measurements are used in the control of several industrial processes, such as the manufacture of adhesives, pectin jellies, starch sponges, and dextrins; in the preparation of foods; and to a more limited extent in the paper and textile industries. They are also frequently used in studies of the granular structure of starches and in determinations of the effects of acids, heat, aging, alcohols, polyhydrols, and other physical or chemical factors on the elasticity of starch and gelatin gels.

The paste wall of most dry cells consists of a mixture of starch and flour in the form of an aqueous gel. Recently the Bureau has made studies of the paste-wall separator of dry cells of the Leclanche type. Gel-strength measurements were used to differentiate walls of different starches, to find out whether the paste reacted with the other constituents of the cell, and to determine the effects of chemical and physical modifications on the strength of the paste wall. The results were correlated with the shelf life of dry cells made with the various types of paste walls.

The characteristics of the paste walls are often described in terms of gelling temperature of the paste or the variety and amount of starch and flour used in its preparation. Frequently the viscosity of the paste is also used for this purpose. For quantitative results, however, a more sensitive method is needed, preferably one that may be used with the gels themselves rather than the pastes from which they are formed. Numerous procedures have been proposed for objective measurements of gel strengths. Several of these are limited in application, because they depend on the breaking or compression of the surface of the gel and are subject to errors owing to skin formations of variable thickness. Furthermore, many methods give a measure of different characteristics of a gel depending upon the point of view of the experimenter. For example, they may indicate rigidity, elasticity, plastic viscosity, or resistance to some force such as cutting action or torsion. The new method developed at the Bureau gives consistent results, well adapted to use in the Bureau's studies of the paste walls of dry cells.

V.2
194

THE FRANKLIN INSTITUTE.

STATED MONTHLY MEETING, WEDNESDAY, DECEMBER 17, 1947.

The stated monthly meeting of The Franklin Institute was held on Wednesday, December 17, 1947, at 8:15 P.M. The President, Mr. Richard T. Nalle, presided over the meeting. The President announced that the minutes of the stated monthly meeting for October were printed in full in the November issue of the JOURNAL OF THE FRANKLIN INSTITUTE, and if there were no corrections or additions, the minutes would stand approved as read. The minutes were approved.

The President then called on the Assistant Secretary, Dr. Frazer, for his report and announcements. Dr. Frazer announced that the following members had been elected during the month of November:

Sustaining	1
Active	30
Associate	19
Student	8
Total membership as of November 30	5417

Dr. Frazer then made the announcement of our Christmas Week Lectures, which are given for young people through the James Mapes Dodge Foundation. It was announced that these lectures would be held on December 30th and 31st at 4:30 P.M., and that the speaker this year would be Mr. Vincent J. Schaefer, who would speak on "Scientific Fun in the Fields, the Mountains, and the Sky."

Dr. Frazer further announced that according to the By-Laws, Article IV, Section 5, nominations for the Board of Managers were to be made at this December meeting. The following members of the Board of Managers, to serve for a period of three years, were nominated:

HIRAM S. LUKENS
ORUS J. MATTHEWS
MORTON GIBBONS-NEFF
CHARLES S. REDDING
GEORGE WHARTON PEPPER
M. M. PRICE
JAMES S. ROGERS
CLARENCE TOLAN, JR.

The President then called for any nominations from the floor. Since no nominations were made, the President announced that the nominations for members of the Board of Managers were closed.

The President then presented the speaker of the evening, Dr. Donald H. Andrews, Professor of Chemistry at the Johns Hopkins University, in Baltimore, Maryland. Dr. Andrews spoke on "Radio and Infra-red Detection by Superconductivity." Dr. Andrews demonstrated a new type of bolometer, which was developed during the recent war at the Johns Hopkins University. The bolometer was used for detecting infra-red rays. It consists of a small ribbon of columbium nitride cemented to the top of a copper block 1 cm. square and 1 cm. high. When cooled to −258.5° C., the ribbon becomes partially superconducting and detects both infra-red and radio waves with a sensitivity in many ways superior to any other known device. Recordings of various kinds of signals received by the bolometer were demonstrated both with an oscilloscope and a loud speaker.

After Dr. Andrews' very edifying lecture, the President adjourned the meeting with a rising vote of thanks to the speaker.

JOHN FRAZER, *Assistant Secretary.*

NEW MEMBERS OF THE FRANKLIN INSTITUTE ELECTED JUNE 1, 1947 TO DECEMBER 1, 1947.

SUSTAINING MEMBERS.

Mr. Sherman Mills Fairchild

Mr. Eugene J. Houdry

ACTIVE MEMBERS WITH FAMILY PRIVILEGES.

Mr. Pierre Aureli
Mr. N. Newlin Baily
Mr. Robert W. Barker
Mr. Mayer I. Blum
Mr. Elmer J. Boetefuer
Mr. Edward G. Budd, Jr.
Mr. Emil Cohn, Jr.
Mr. John M. Diem
Mr. Moses Ehrlich
Mr. Joseph H. Gillies
Mr. Charles H. Godschall
Mr. Harry C. Hambridge
Mr. Harry R. Hirshorn
Mr. David H. Hopkins
Mr. Laurence T. Howell
Mr. Edward Kohlhepp
Mr. George Lipsky
Mr. John S. Malick
Mr. John Cochrane Martin
Mr. John F. McNelis
G. Herbert Moffses, M.D.
Mr. Harry E. Mousley
Mr. Robert Nagel
Mr. Gordon Null
Mr. Marvin H. Pond
Mr. Howard C. Pruyn
Mr. Harry Rubin
Mr. Theodore A. Seraphin
Mr. Samuel A. Weston
O. Wilson Winters, D.D.S.
Mr. Carl A. Wolf

ACTIVE MEMBERS.

Mr. William Loughridge Aiken
Mr. Edward J. Bailey
Major General Milton G. Baker
Mr. Henry S. Bamford
Mr. Naaman F. Barr
Mr. William L. Baumner, Jr.
Mr. Charles W. Berg
Mr. Sanford Bliwise
Mr. Lou Block
Mr. M. A. Bordman
Mr. Harry S. Boud
Mr. John E. Bower
Mr. William H. Brearley, Jr.
Mr. W. Ronald Briggs
Mr. Harold W. Brown
Mr. James M. Castle
Mr. George A. Clickenger
Mr. Frank G. Conrad, Jr.
Mr. Edward F. Cooper
Mr. Edward P. Cornely
Mr. George J. Crits
Mr. Joseph Croskey
Mr. E. B. Curdts
Mr. Edwin A. Dages
Mr. Joseph De Frenes
Mr. William J. Devinney
Mr. Felix Di Arenzo
Mr. Ralph Earle
Mr. A. J. Ellis
Mr. Jay Emanuel
Paul J. Ernst, Ph.D.
Mr. Woodfin R. Fagge
Mr. William F. Famille
Mr. Mort F. Farr
Mr. Myer Feinstein
Mrs. Jeanne Ferber
Mr. Alex C. Fergusson
Mr. Harry B. Fertik
Thomas Fitz-Hugh, Jr., M.D.
Mr. Lawrence S. Ford
Mr. John J. Fox
Mr. Benjamin H. Freeman
Mr. Charles H. Fryburg
Mr. Edward E. Gallob
Mr. Arthur S. Gleason
Mr. Richard A. Griefen
Mr. H. K. Groff
Mr. William P. Groves, Jr.
Mr. Amil S. Gumula
Mr. Fred C. Haab
Mr. Joseph J. Hagan
Mr. Wilson C. Hanline
Mr. Paul V. Hannas
Mr. Abdullah Feyzi Hamdi
Mr. W. J. Heggie
Mr. Robert F. Herr
Gerald E. Herrnstadt, Ph.D.
Mr. Emil Hoffman
Mr. William P. Hood
Mr. William Hopkin
Mr. Wayne L. Hopkins
Mr. John J. Howard
Mr. A. D. Howry
Mr. Robert V. Hudson
Mr. Joseph Gray Jackson
Mr. Bernard Jacobs
Mr. C. Brooke Jones
Mr. Morris Katz
Mr. John Keefe, Jr.
Mr. John Kerbeck
Mr. Ellis Knowles
Mr. William Kolb
Mr. Alfred Theodore Kornfield
Mr. Ellis M. Landis
Mr. Henri Lauer
Miss Dorothy K. Lawrence
Mr. Hurley Lazarus
Mr. Alfred Leith
Mr. Adam Leva
Norton M. Levin, D.O.
Mr. Willard F. Levy
Mr. Joseph F. Lewis
Mr. John Franklin Long
Mr. Thomas C. Longstreth
Mr. James Luckman
Mr. Lionel P. Maggenti
Mr. Charles W. Maloney
Mr. John Mallo
Mr. Thomas I. Manly
Mr. Samuel A. Mann
Mr. Vernon L. Marquart
Mr. Emil A. Mathias
Mr. T. E. McBride
Mr. Laurence T. McCurdy
Mr. Sterling R. Mensch

Mr. C. B. Miller
Mr. Raymond Millman
Mr. Harry W. Morgan
Mr. Robert V. Morris
Mr. Richard J. Mott
Mr. Arthur Niessen
Mr. Charles H. Nonamaker
Mr. M. John O'Donoghue
Mr. Gordon Palmer, Jr.
Mr. Daniel C. Parr
Mr. Edward Paul
Mr. Richard D. Pomerantz
Mr. Clarence H. Porter
Mr. F. B. Powers
Mr. Harold C. Rahn
Mr. Leonard Rodenhausen
Mr. Frank B. Russell
Mr. Herman Schaevitz
Harold G. Scheie, M.D.
Mr. Morris Schiff
Mr. Frederick J. Schneider
Mr. Howard I. Scherr
Mr. Gerry W. Schulz
Mr. Richard Schweder
Mr. Robert D. Scott
Mr. Louis Segal
Mr. John B. Shields
Mr. Chao Tze Shih
Dr. Alfred R. Smith
Mr. Cortland Gray Smith
Mr. Edward W. Smith, Jr.
Mr. Perry C. Smith
Mr. Albert Soffa
Mr. Robert Solts, Jr.
Mr. Ulrich Sontheimer
Mr. James C. Stambaugh
Mr. Albert D. Stave
Mr. Saul H. Steel, Jr.
Dr. John A. Stevenson
Mr. Charles M. G. Stewart
Mr. E. Lee Strock
Mr. Lisle J. Sykes
Mr. John J. Townsend
Mr. John W. Temple
Mr. John M. Tinker
Mr. Irving S. Towsley
Mr. Wilmer S. Trinkle
Mr. William A. Tucker
Mr. Russel R. Tull
Mr. Edward S. Turner
Mr. Ralph Vezin
Mr. Alfred M. Whitney
Mr. Edward J. Williams
Mr. R. M. Wilson
Mr. Samuel S. Wolfman
Mr. R. E. Worden
Carroll S. Wright, M.D.
Mr. Joseph A. Wurster, Jr.
Mr. Samuel M. Zollers

ACTIVE NON-RESIDENT MEMBERS.

Mr. George W. Alcock
Mr. Carleton Craig
Mr. John R. Heizmann
Mr. Arthur T. Hinckley
Mr. Mortimer Francis Nahon
Mr. Guy F. Rolland
Mr. P. A. Shields
Mr. George H. Woodard

NECROLOGY.

Mr. Charles S. Beach '01
Miss Elizabeth C. Biddle '09
Mr. C. H. Bierbaum '97
Mr. George Imlay Bodine, Jr. '44
Mr. Julius Boekel '84
Mr. Franklin S. Chambers '41
Mr. Robert Cherry, Jr. '37
Mr. Morris L. Clothier '26
Mr. Walter T. Dwyer '46
Mr. Charles J. Eisenlohr '36
Mr. William M. Elkins '42
Mr. John J. Foulkrod, Jr. '36
Mr. William H. Frey '43
Mr. Anthony H. Geuting '36
Mr. John Elgin Gilmer '43
Mr. Joseph Handler '43
Mr. Frederick A. Healy '36
Boyden W. Kowalski, M.D. '44
Mr. John M. Krupp '43
Mr. James Barton Longacre '38
Mr. Sylvester A. Mahan '46
Mr. James T. J. Mellon '42
Samuel Nicholas, M.D. '44
Max Planck, Ph.D. '27
Mr. J. Benton Porter '41
Mr. Paul C. Richter '46
Mr. Isaac B. Ritter '42
Mr. Charles E. Schmidt '43
J. E. Shrader, Ph.D. '22
Mr. J. Stogdell Stokes '36
Mr. S. M. Swaab '46
Mr. Henry F. Wageman '46
Miss Hepsey Norris Wells '34
Mr. William H. B. Whitall '36
Thomas L. Wilcox, D.D.S., '45
Major Richard R. Wright, Sr. '46

COMMITTEE ON SCIENCE AND THE ARTS.

(Abstract of Proceedings of Stated Meeting held Wednesday, November 12, 1947.)

HALL OF THE COMMITTEE,
PHILADELPHIA, NOVEMBER 12, 1947.

MR. WALTER C. WAGNER in the Chair.

The following report was presented for final action:

No. 3186: Henderson Medal.

This report recommended the award of a George R. Henderson Medal to Charles Duncanson Young, of Whitford, Pennsylvania, "In consideration of his contributions to the

scientific advancement of the steam locomotive which has resulted in improving the reliability and efficiency and reducing the cost of steam locomotives thereby producing a more effective transportation unit."

(Abstract of Proceedings of Stated Meeting held Wednesday, December 10, 1947.)

HALL OF THE COMMITTEE,
PHILADELPHIA, DECEMBER 10, 1947.

MR. WALTER C. WAGNER in the Chair.

The following report was presented for final action:

No. 3185: Electrical Gun Director.

This report recommended the award of a Howard N. Potts Medal each to David Bigelow Parkinson, of Maplewood, New Jersey, and Clarence Anding Lovell, of Summit, New Jersey, "In consideration of their combined contributions, both to the theoretical and practical design of the Electrical Gun Director, one of the outstanding pieces of equipment developed during the war period, which development has further contributed largely to the theory and practical application of servo mechanisms and smoothing filters in general."

JOHN FRAZER,
Secretary to Commmittee.

LIBRARY NOTES.

The Committee on Library desires to add to the collections any technical works that members would wish to contribute. Contributions will be gratefully acknowledged and placed in the library. Duplicates received will be transferred to other libraries as gifts of the donor.

Photostat Service. Photostat prints of any material in the collections can be supplied on request. Orders received in the morning are filled the same day. The average cost for a print 9 × 14 inches is thirty-five cents.

The Library and reading room are open on Mondays, Tuesdays, Fridays and Saturdays from 9 A.M. until 5 P.M., Wednesdays and Thursdays from 2 P.M. until 10 P.M.

V.2
194

RECENT ADDITIONS.

BACTERIOLOGY.

HINSHELWOOD, C. N. The Chemical Kinetics of the Bacterial Cell. 1946.

CHEMISTRY AND CHEMICAL TECHNOLOGY.

CHEMICAL RUBBER COMPANY. Handbook of Chemistry and Physics. Thirtieth Edition.
COLLOID SCIENCE. A Symposium. 1947.
DORÉE, CHARLES. Methods of Cellulose Chemistry Second Edition. 1947.
EASTMAN, E. D., AND G. K. ROLLEFSON. Physical Chemistry. 1947.
EITEL, WILHELM. Physikalische Chemie der Silikate. 1941.
HEATON, NOEL. Outlines of Paint Technology. Third Edition. 1947.
KNAGGS, NELSON S. Adventures in Man's First Plastics. 1947.
KOLTHOFF, ISAAC, AND V. STENGER. Volumetric Analysis. Second Edition. Volume 2. 1947.
MANTELL, CHARLES L. The Water-soluble Gums. 1947.
PIETERS, H. A., AND D. W. VAN KREVELEN. The wet Purification of Coal Gas and Similar Gases. 1946.
PRICE, CHARLES C. Mechanics of Reactions at Carbon-Carbon Double Bond. 1946.
REMINGTON, JOHN STEWART. Pigments. 1944.
SCHMIDT, J., AND H. G. RULE. A textbook of Organic Chemistry. Fifth Edition. 1947.
SOMMER, HUGO HENRY. The Theory and Practice of Ice Cream Making. Fifth Edition. 1946.
THIENE, HERMANN. Glas. Volumes 1 and 2. 1931 and 1939.

ELECTRICITY AND ELECTRICAL ENGINEERING.

BARROWS, E. J. Industrial High Voltage. Distribution and Public Supply. 1946.
CULVER, CHARLES AARON. Theory and Applications of Electricity and Magnetism. 1947.
L'HERMITE, ROBERT. L'experience et les Théories Nouvelles en Resistance des Matériaux. 1945.
LAURSON, P. G., A. MERRILL, AND W. JAMES. Elements of Mechanism. Second Edition. 1947.
ORCHARD, FREDERICK C. Electricity in the Building Industry. 1946.
SLATER, J. C., AND N. H. FRANK. Mechanics. 1947.
WALL, T. F. ELECTRICAL ENGINEERING. 1947.

INDUSTRIAL MANAGEMENT.

TREWMAN, HARRY F. Mechanical Inspection. 1946.

MATHEMATICS.

HOEL, PAUL G. Introduction to Mathematical Statistics. 1947.
MARSHALL, W. R., AND R. L. PIGFORD. Application of Differential Equations to Chemical Engineering Problems. 1947.

METALLURGY.

BREARSLEY, HARRY. Talks About Steelmaking. 1946.
CHESTER, J. H., AND M. W. THRING. Influence of Port Design on Open-Hearth Furnace Flames. 1946.
JENKINS, IVOR. Controlled Atmospheres for the Heat Treatment of Metals. 1946.
NELSON, J. H. AND H. SILMAN. The Application of Radiant Heat to Metal Finishing. 1945.
WOOD, V. N. Metallurgical Materials. 1946.

OPTICS.

TOLANSKY, S. High Resolution Spectroscopy. 1947.

PHOTOGRAPHY.

DISERENS, CHARLES. Handbuch der Photographie. Volume 1. No date.
DISERENS, CHARLES. Traite de Photographie. Volume 1. 1943.
MORGAN, W. D., H. M. LESTER AND OTHERS. Graphic Graflex Photography Eighth Edition. 1947.

PHYSICS.

MICHENER, WILLIAM H. Physics for Students of Science and Engineering. 1947.
MORSE, F. T. Elements of Applied Energy. 1947
SLATER, J. C., AND N. H. FRANK. Mechanics. 1947.
WEBER, R. L., M. W. WHITE, AND K. V. MANNING. College Technical Physics. 1947

RADIO.

HARRISON, ARTHUR EDWARD. Klystron Tubes. 1947.

SCIENCE.

HALDONE, J. B. S. Science Advances. 1947.
HEATH, H. F., AND A. L. HEATHERINGTON. Industrial Research and Development in the United Kingdom. 1946.

NOTES FROM THE BIOCHEMICAL RESEARCH FOUNDATION.

Enzymatic Hydrolysis of Desoxyribonucleic Acid Prepared with the Use of Strong Sodium Hydroxide.—CHARLES A. ZITTLE. It was previously reported (1) that desoxyribonucleic acid (DNA) prepared under mild conditions (method of Hammarsten) (2) was readily hydrolyzed by specific nuclease so that it became soluble in HCl, whereas DNA prepared with the use of hot 1.25 N NaOH (method of Levene) (3) was not hydrolyzed by the nuclease. Further study has shown that under the proper conditions the alkali-treated DNA can be slowly hydrolyzed by the nuclease at a rate about 20 per cent. of that of DNA (Hammarsten). The previously reported erroneus conclusion that DNA (Levene) could not be hydrolyzed was in consequence of this low rate of hydrolysis and the instability of the enzyme under the conditions used.

Experimental.

Preparation of the enzymes and substrates and the manometric and other procedures have been described (4). In initial experiments with DNA (Hammarsten) this nucleic acid was contemplated as a substrate for the phosphoesterase from calf intestinal mucosa (5), and for this purpose it was treated with specific nuclease since hydrolysis of DNA by the phosphoesterase is only rapid and complete after it has been acted on by specific nuclease (4). For preparing the nuclease-treated DNA the nuclease was obtained in the form of a dried ammonium sulfate precipitate and weighed amounts of this material were added directly to the nucleic acid soultions. The above observations about hydrolysis were made under these conditions. In subsequent attempts to use dilute solutions of the nuclease in manometric experiments it was found to be very unstable, but could be stabilized by the addition of neopeptone following observations of McCarty (6).

A stable nuclease solution was prepared as follows: 300 mg. were dissolved in 20 cc. of 0.0005 N H_2SO_4 and dialyzed against the same to remove the ammonium sulfate; 6.0 cc. of this solution were mixed with 4.0 cc. of neutralized neopeptone, 1.3 cc. of 0.5 M $NaHCO_3$ and 0.7 cc. of 0.3 M magnesium chloride. This solution, prepared from the dialyzed enzyme for each experiment, was used in the experiments to be described.

The initial rates of hydrolysis of the two nucleic acids were determined manometrically. In each experiment 2.0 cc. of 0.6 per cent. nucleic acid together with 0.2 cc. of 0.5 M $NaHCO_3$, variable amounts of enzyme in the side arm of Warburg flasks, and water to make the

final volume 3.5 cc. were used. In these experiments the initial rates of hydrolysis were: for DNA (Hammarsten), 91.2 cmm./10 min./1.0 cc. of nuclease; for DNA (Levene), 17.0.

Precipitates obtained by acidifying solutions of DNA (Levene) with HCl turn a light brick red on standing for some time; initially the precipitates are white. This observation and the slow rate of hydrolysis of this nucleic acid suggested that an inhibitory substance might be present from the reagents (colloidal iron, for example) used in its preparation. Hydrolysis of the two preparations of nucleic acid in the same flask (followed manometrically: 6.0 mg. of each nucleic acid, 0.5 cc. of enzyme), however, was equal to the sum of the two taken alone, indicating that the alkali-treated nucleic acid preparation was not inhibitory to hydrolysis of the other. With the same thought in mind the alkali-treated nucleic acid was dialyzed for 24 hours, precipitated with HCl (final concentration, 0.24 N; pH 1.2) and dried with acetone. Fifty-eight per cent. of the starting material were recovered. The enzymatic hydrolysis of this material (followed manometrically: 3.0 to 9.0 mg. of nucleic acid; 0.5 cc. enzyme), however, was the same as that of the original.

For complete hydrolysis of the alkali-treated nucleic acid at 23°, measured by solubility in 0.25 N HCl, the following procedure was adequate. Nine parts of 0.6 per cent. solution of the nucleic acid were treated with successive portions of the enzyme solution: with two parts initially, with two parts at the end of 4 hours, and with two parts at the end of 7 hours. The last portion of enzyme was permitted to act for 18 hours with the solution saturated with chloroform. Although precipitation with HCl was now negative, precipitation with the uranium reagent had remained unchanged.

Phosphoesterase was permitted, as was done previously (1), to act on the above digest without and with silver nitrate present, the silver to inhibit the adenosine deaminase in these preparations. With this complete digest the results are comparable to those obtained with digest of DNA (Hammarsten); with silver present more CO_2 is released due to the inhibition of the deaminase and consequent production of ammonia. This is in contrast to previous results with DNA (Levene). From the previous results it was difficult to decide whether the DNA had been deaminated by the strong alkali used in its preparation or that the phosphoesterase had not liberated adenosine. From the present data it appears that the latter explanation was the correct one.

Discussion.

The previous observation (1) that DNA (Levene) was not hydrolyzed was made because of the instability of the enzyme under the conditions used and also because of the low rate of hydrolysis of this prepation of nucleic acid. The DNA (Hammarsten) was rapidly hydrolyzed

and hydrolysis was complete before the activity of the enzyme was lost, but, the DNA (Levene) showed little or no hydrolysis during the same period of time. The results of the present study indicate that adenosine deaminase can act on both of these hydrolysates and there is no reason for believing that the adenine radical is involved in the low rate of hydrolysis.

Summary.

In contradiction to results previously reported, it has been found that DNA prepared by a method which utilizes strong NaOH is acted on by the specific nuclease, although at a rate only 20 per cent. of that of DNA prepared by a milder method. The nature of the changes responsible for the low rate of hydrolysis of the alkali-treated DNA are not known.

References.

(1) ZITTLE, C. A., *J. Franklin Inst.*, **243**: 334 (1947).
(2) HAMMARSTEN, E., *Biochem. Z.* **144**: 385 (1924).
(3) LEVENE, P. A., *J. Biol. Chem.*, **53**: 441 (1922).
(4) ZITTLE, C. A., *Arch. Biochem.*, **13**: 191 (1947).
(5) ZITTLE, C. A., *J. Biol. Chem.*, **166**: 491 (1946).
(6) MCCARTY, M., *J. Gen. Physiol.*, **29**: 123 (1946).

V.2
194

BOOK REVIEWS.

AIR CONDITIONING AND ELEMENTS OF REFRIGERATION, by Samuel P. Brown. First Edition. 644 pages, drawings and illustrations, 15 × 23 cms. New York and London, McGraw-Hill Book Co., Inc. 1947. Price $6.00.

"The objective of this book is to provide a complete, practical, working textbook and handbook suitable for the study by any interested person and to those working in design, installation, operation of heating, ventilating, and other mechanical equipment of buildings." The selection of equipment, automatic controls, and design of air ducts and liquid piping systems are covered, as well as refrigeration theory.

The tables necessary for elementary design work are included, although complex theory and higher mathematics have been eliminated.

Throughout the text, illustrative practical problems are presented, which are then answered in the appendix. There are over 230 graphs and illustrations throughout the book.

HENRY E. MICHAEL.

FUNDAMENTALS OF ELECTRICITY AND MAGNETISM, by Leonard B. Loeb. Third Edition. 669 pages, drawings, 15 × 24 cms. New York, John Wiley & Sons, Inc., 1947. Price $6.00.

This textbook, originally written to fill a specific need at the University of California, presents the subject, in its third edition, as a consistent and related whole, rather than isolated and dogmatically stated topics.

The historical survey of previous editions is replaced by a brief historical outline and the space thus gained is devoted to the enlargement of the section on atomic structure.

The book begins with elementary magnetism and direct current electricity followed by the study of static electricity. The c.g.s. is utilized, since it is felt by the author that electricity, basically so closely associated with electronic and atomic phenomena, profits more from its use rather than the m.k.s. system, which has its advantages in application to gross mechanics or engineering physics.

HENRY E. MICHAEL.

TABLES OF INTEGRALS AND OTHER MATHEMATICAL DATA, by Herbert Bristol Dwight. Revised edition. 250 pages, tables, 14 × 21 cms. New York, The Macmillan Co., 1947. Price $2.50.

This book contains a variety of mathematical data in formula and tables including algebraic, trigonometric, inverse trigonometric, exponential, logarithmic, hyperbolic, inverse hyperbolic, elliptic, and Bessel functions. There are also probability integrals, surface zonal harmonics, definite integrals and differential equations. An appendix gives tables of numerical values and a list of 62 references referred to in the text where the derivation of the results is given and where further results may be found. At the end of the book there is also a subject index giving more details on material location so that for instance gamma function or Bernoulli's numbers may be found quickly. This second addition of this work is a convenient tool for those who use mathematics to any extent.

R. H. OPPERMANN.

THE CHEMISTRY OF COMMERCIAL PLASTICS, by Reginald L. Wakeman. 836 pages, tables and illustrations, 15 × 24 cms. New York, Reinhold Publishing Corporation, 1947. Price $10.00.

Twenty years ago it was not uncommon to hear it said that all pioneering in organic chemistry was over—organic chemistry was no longer a virile science for no discoveries of fundamental importance had been made by its devotes since the brilliant éclat of the aniline dye

industry. But the foundations were being laid for a new glorious period for organic chemistry, the Age of Plastics. Plastics, as we know them today, cover a large group of organic substances, either wholly or in part synthetic, which can be molded into coherent solid articles that retain their shape indefinitely at room temperature. This book is an analysis of the fund of information on the subject which correlates the scientific data with actual present industrial practice.

After an introductory chapter and a reference to the history of the plastics industry the work examines in a general way some of the relationships which exist between the various raw materials and the plastics made from them. This leads to treatments on general chemical principles of resinification and ways in which synthetic resins and plastics are manipulated in making diverse products. Thereafter consideration is given separately to specific subjects such as phenolic, urea and melamine plastics, aniline-formaldehyde resins, polyamides-nylon, coumarone-indene resins, polyvinylidene chloride, polystyrene, rubber derivatives, natural and synthetic elastomers, cellulose, lignin and protein plastics, polymeric organosilicon-oxygen compounds. These represent the most important plastics of commerce. There have been developed many other synthetics of more or less resinous character and are marketed for special purposes in relatively small volumes. Some of these are taken up in the last chapter together with a few which have been studied extensively in industrial laboratories but which still have not appeared on the market. In the back of the book there is an author and a large well arranged subject index.

This book is the result of an exhaustive survey of the literature and an intimate knowledge of the industry. The many illustrations, tables, curves, diagrams coupled with skill in presentation and a progression to present practice pointing to the future make this book a valued contribution to the literature as a text and reference work.

R. H. OPPERMAN.

TEXTILE FIBERS by J. M. Matthews and H. R. Mauersberger. Fifth Edition. 1133 pages, tables and illustrations, 15 × 24 cms. New York, John Wiley & Sons, Inc., 1947. Price $12.50.

The history of fiber development has been a strange pattern of trial and error ever since fibers were first used for making apparel. Climate had much to do with it since wool, hair and fur fiber had great and continual development in cold climates and in hot climates development was first found in vegetable fibers. With the invention of machinery, fiber development was more rapid. Some fibers were delayed in development because of man's inability to dye them satisfactorily and to degum with sufficient thoroughness. Then came the need, particularly of the totalitarian nations, of producing ersatz materials to take the place of natural fibers. New methods, new products, new machines, and new techniques continually displace the old. This volume on fibers depicts the progress that has been made in textile fibers, their economic utilization, and technical development.

Now in its fifth edition, the book has 1095 pages of text, written for the student in colleges and technical school and as a reference for those who deal with the sale, production, processing, and conversion into fabric of all the different fibers now used in the textile and clothing industries. A suitable introduction leads into a general detail of the essential physical, microscopic, and chemical properties which make fiber a valuable textile material. Later, these properties are given considerable space with regard to cotton, the bast fibers, structural or hard vegetable fibers, wool, specialty hair fibers, silk, rayon, new synthetic textile fibers, and material or inorganic fibers and filaments. A complete coverage is given including the economics, production, cultivation, statistics, prices, dyeing, spinning, etc. A considerable section is devoted to fiber identification methods, the quantitative determination of fibers present in a product, and fiber testing methods. There is a bibliography at the end of each of the 24 chapters and in the back of the book there is a large comprehensive subject index.

This monumental work is the sum of the work of forty-six contributors, collaborators and reviewers whose work was supervised in selection, revision and arrangement by an editor with much experience in the industry. It is of practical value today and points to fields of research and promise for the future.

R. H. OPPERMANN.

SERVOMECHANISM FUNDAMENTALS, by Henri Laurer, Robert Lesnick, and Leslie E. Matson. First Edition. 277 pages, drawings, 16 × 23 cms. New York and London, McGraw-Hill Book Co., Inc., 1947. Price $3.50.

The term "servomechanism" is generally used to denote a particular class of automatic control system where the controlling signals of the system change fast and frequently. This type of system is different from the "regulator" in that in the case of the regulator the controlling signals do not change or change slowly and the primary problem is to prevent extraneous causes from affecting the function controlled by the system. Servomechanisms are used to steer ships, control airplanes, automatically tune radio receivers, position guns, etc. Regulators control temperatures, maintain liquid levels etc. This newer servomechanism principle has the outstanding features that the controlled and controlling elements of the system may be widely separated, that the work performed may be many times greater than required for control operation and the often complicated processes can be made to take place according to predetermined standards.

This book is designed for practicing engineers as an introduction to the principles underlying the theory of servomechanisms. As such it starts with the elements and proceeds to the more complex with sympathy to the needs of those who require refreshing or review coverage on many forgotten subjdcts. In detail, the work begins with defining the concepts of control of open and closed control systems and the means employed for accomplishing control operations. Simple practical examples are described, enough to give an idea of duties performed which could hardly be accomplished by other means. The servo system follow up link; a differential device which produces an indication of the magnitude and direction of the error between the input and output members of the system, is next taken up.

Because servo-control systems involve a knowledge of both mechanical and electrical engineering principles, the authors have inserted at this point a chapter on fundamentals of mechanics and electricity as a review covering only the most elementary concepts. Then proceeding onward the book treats on principles of the transient analysis method of elementary servomechanisms. This is divided as follows: analysis of servomechanisms with viscous output damping, with error rate damping, with combined viscous output damping and error-rate damping, with integral control, and an enlargement in greater detail devoted to practical means for obtaining error rate damping, and a discussion of error rate stabilization networks. There is an introduction to the transfer function analysis of servomechanisms which is a frequency analysis and the relation of this to the transient analysis is indicated. The last chapter of the book is devoted to typical design calculations and general consideration. At the end there is a subject index.

The practicing engineer who has a need of familiarity with servomechanisms will find in this book a useful tool.

R. H. OPPERMANN.

PETROLEUM PRODUCTION, by Park J. Jones. Volume III. 271 pages, 16 × 24 cms., tables and drawings. New York, Reinhold Publishing Corporation, 1947. Price $5.00.

This is Volume III of a series of books and is limited to oil production by water. This excludes primary gas caps and oil production by gas. The book is divided into two parts, the first dealing with foundations. Essentially in the form of a text, formulas, curves, and charts are given with discussions on reservoir space in barrels, the fluid factor and its effects, oil production by expansion, well producing capacity and the factors effecting it, injection of water, the optima for reservoirs involving economical as well as physical factors, and the migration of oil. Part two of the book is on applications and its coverage includes discussions on radial reservoirs, two pay intervals, impermeable wedges, saturated oil, linear reservoirs, elongated reservoirs, and bottom water. A subject index is in the back.

The presentation shows a practical application of facts and figures relating to this type of petroleum production.

R. H. OPPERMANN.

PUBLICATIONS RECEIVED.

The Chemistry and Technology of Waxes, by Albin H. Warth. 519 pages, drawings, tables and illustrations, 15 × 23 cms. New York, Reinhold Publishing Corporation, 1947. Price $10.00.

Architectural Construction, by Theodore Crane. 414 pages, drawings and illustrations, 16 × 25 cms. New York, John Wiley & Sons, Inc., 1947. Price $6.00.

Field Practice, by Elwyn E. Seelye. A Data Book for Civil Engineers. 306 pages, tables and drawings and illustrations, 13 × 21 cms. New York, John Wiley & Sons, Inc., 1947. Price $4.50.

Saga in Steel and Concrete, by Kenneth Bjork. 504 pages, 16 × 24 cms. Northfield, Norwegian-American Historical Association, 1947. Price $4.00.

Industrial Health Engineering, by Allen D. Brandt. 395 pages, drawings, tables and illustrations, 15 × 24 cms. New York, John Wiley & Sons, Inc., 1947. Price $6.00.

Flight Engineering and Cruise Control, by Harris G. Moe. 209 pages, drawings and illustrations, 15 × 23 cms. New York, John Wiley & Sons, Inc., 1947. Price $4.00.

Very High-Frequency Techniques, compiled by the staff of the Radio Research Laboratory, Harvard University. Volumes I and II. First Edition. 554 pages, and 1057 pages, drawings and illustrations, 16 × 24 cms. New York, McGraw-Hill Book Co., 1947. Price $14.00, two volumes.

The American Annual of Photography 1948, edited by Frank R. Fraprie and Franklin I Jordan. 216 pages, illustrations, 18 × 25 cms. Boston, American Photographic Publishing Co., 1947. Price $2.00.

Chemical Engineering Fundamentals, by Chalmer G. Kirkkride. 419 pages, tables and drawings, 15 × 24 cms. New York, McGraw-Hill Book Company, Inc., 1947. Price $5.00.

CURRENT TOPICS.

Detecting Impurities in Uranium. (*Electrical Engineering*, Vol. 66, No. 7.)—Thirty-three impurity elements, some in concentrations as low as one part in 20 million, have been detected and estimated through a modified spectrographic method developed at the National Bureau of Standards and used since 1942 in the Manhattan Project for analysis of uranium and its compounds.

Impurities differ in their effects on the nuclear chain reaction. Some elements such as boron and cadmium may interfere if present in concentrations as low as a few tenths of a part per million, and many other elements should not exceed a few parts per million. Rapid, sensitive, and accurate methods therefore are required for the determination of at least 60 chemical elements in a variety of uranium-base materials. Established spectrographic methods of analysis are unsuccessful because of interference by the complex uranium spectrum in which more than 20,000 lines have been observed.

This difficulty was overcome by separating the impurities from the uranium in the carrier-distillation method by converting the uranium sample to a refractory compound having low volatility (the black oxide of uranium U_3O_8) and distilling the impurities from this compound in a d-c electric arc.

In order to sweep out the minute quantities of impurity vapors from the sample without volatilizing the uranium, a small amount of a volatile material, termed a "carrier," is added to the sample. Gallium oxide was found most useful as a carrier and is added at a concentration of two per cent in the uranium oxide. When the mixture is heated by a d-c arc in a carbon electrode of special design, the carrier material and impurities are volatilized into the arc. The uranium, remaining as a residue, can be recovered readily from the electrode—an important consideration, particularly with some active forms of uranium. The light of the arc, examined with a spectrograph, provides a spectrum consisting of the simple spectrum of gallium plus the spectral lines characteristic of volatile impurities in the uranium.

For quantitative determinations, carefully prepared standards of known composition are submitted to the same treatment as the samples. Amounts of impurities are then estimated by photometric measurement, or by visual comparison of the spectrograms of samples and standards. Determinations are made to an accuracy of plus or minus 10 per cent of the amount of the element present. For example, boron and cadmium can be observed easily at a concentration of 1 part in 10 million, and the concentration can be determined to within one tenth of this amount. The greatest sensitivity, observed for the detection of silver, was 1 part in 20 million.

R. H. O.

Stand Built to Test Governors Under Service Conditions. (*Compressed Air Magazine*, Vol. 52, No. 6.)—Governors for diesel engines must be built with accuracy to perform the important function for which they are designed. These units control the amount of fuel injected into the engine cylinders by

the fuel pumps and come into action as soon as the engine overspeeds or underspeeds. In many cases where diesels drive equipment such as electric generators, governors must be extremely sensitive to slight changes in engine speed, and it is for this reason that they have to undergo rigid testing and minute adjustment under simulated running conditions before they leave the factory. This applies not to one unit picked at random from a lot but to each one, and has led the Woodward Governor Company to design and construct a test stand that does this work not only in routine fashion but also with precision.

The stand consists of a cast-iron surface plate and pedestal and is equipped with an air motor of the Multi-Vane Type that has a speed range from 150 r.p.m. to 4200 r.p.m. This unit drives the governor which, in turn, controls the speed of the motor by throttling the air supply. Air at from 80 to 100 p.s.i. is used, and the pressure must be kept constant close to the stand for satisfactory testing.

Different types of governors can be coupled to the motor by means of a mounting plate and drive-shaft adapters, of which three are standard equipment. Depending upon whether it is keyed or serrated, the adapter is either attached to the governor drive shaft or dropped into a flywheel recess in the table top. The shaft is then inserted in the recess until the governor rests squarely upon the flat surface plate, something that is necessary for smooth running. It may also involve moving the motor up or down in order to get it in proper position to drive the shaft.

After the governor has been filled with oil to a predetermined level and been linked with an adjustable fulcrum on the stand, the air motor is started. This is done by flexing the cable that connects the fulcrum and the air-control lever until the governor takes over. Testing involves dispelling all air bubbles by allowing the governor to surge for about five minutes, warming the oil by letting the unit run from 15 to 20 minutes, adjusting the compensating needle valve, and checking the response of the governor under its specified high and low speeds and under other service conditions. Excessive heating, vibration, oil leakage, and defective parts can be detected by the stand operator, and different measuring and indicating instruments enable him to make the corrections and adjustments necessary to insure a governor that will do the exacting work for which it is designed.

R. H. O.